2016

Complex Coacervate-based Materials for Biomedicine

Sarah L. Perry
University of Massachusetts Amherst

Whitney C. Blocher
University of Massachusetts Amherst

Recommended Citation
Perry, Sarah L. and Blocher, Whitney C., "Complex Coacervate-based Materials for Biomedicine" (2016). *WIREs Nanomedicine and Nanobiotechnology*. 835.
https://doi.org/10.1002/wnan.1442

Complex Coacervate-Based Materials for Biomedicine

Authors: Whitney C. Blocher and Sarah L. Perry

Abstract

There has been increasing interest in complex coacervates for deriving and transporting biomaterials. Complex coacervates are a dense, polyelectrolyte-rich liquid that results from the electrostatic complexation of oppositely-charged macro-ions. Coacervates have long been used as a strategy for encapsulation, particularly in food and personal care products. More recent efforts have focused on the utility of this class of materials for the encapsulation of small molecules, proteins, RNA, DNA, and other biomaterials for applications ranging from sensing to biomedicine. Furthermore, coacervate-related materials have found utility as in other areas of biomedicine, including cartilage mimics, tissue culture scaffolds, and adhesives for wet, biological environments. Here, we discuss the self-assembly of complex coacervate-based materials, current challenges in the intelligent design of these materials, and their utility applications in the broad field of biomedicine.

Introduction

Complex coacervation is an associative, liquid-liquid phase separation phenomenon[1-12] that is driven by an initial electrostatic attraction between oppositely charged macroions,[1-5,13-19] followed by the entropic gains associated with the release of small, bound counter-ions and the restructuring of water molecules.[1-3,13] The original work by Bungenberg de Jong focused on biomacromolecular systems of proteins and polysaccharides.[20] Building on this foundational research, coacervates have found utility as encapsulants, additives, emulsifiers, and viscosity modifiers in food science and personal care products.[21-26] The scope of coacervation has expanded from proteins and polysaccharides to include polynucleotides,[7,8,27-30] synthetic polymers,[31-37] surfactants,[38-45] nanoparticles,[46,47] and other hierarchical assemblies.[48-55] Furthermore, the utility of coacervates has extended into fields such as adhesives,[9,56-70] drug delivery,[4,7,8,16-19,28,32,34,71-84] nano/bio-reactors,[31,33,85-87] and cellular biology.[7,88-105]

Much of the utility of coacervates, particularly in the areas of food science, personal care products, and medicine comes from the ability to generate formulations and drive encapsulation in the absence of organic solvents.[3,4,73,106] Coacervation is typically performed directly from aqueous solutions of oppositely charged macro-ions, and is modulated via changes in ionic strength, pH, etc.[1,6,29,55,72,74] The use of naturally-derived biomacromolecules can further facilitate the biocompatibility of the resulting coacervate-based materials,[4,16,73,107,108] although a wide range of safe and highly effective synthetic polymers have also been demonstrated.[4,73,109,110] Alternatively,

materials with innate antimicrobial and/or antibacterial activity such as poly(*L*-lysine) or poly(ethyleneimine) can be taken advantage of for some applications to circumvent the need for additional active ingredients while avoiding the potential for developing antibiotic resistant bacteria.[111-113] Moving beyond the mere use of biological materials, researchers have also drawn inspiration from biological processes such as DNA-histone binding,[28] heparin-growth factor interactions,[19,76-78,107,108,110] and intracellular protein-RNA granules.[82,92,94,101,102] Similarly, coacervate-based materials can be designed to respond to a variety of stimuli, including ionic strength, changes in pH, redox chemistries, temperature, light, etc. for use in sensing[27,114-116] or drug delivery applications.[74,106,117] This review is designed to provide an overview of complex coacervation, with an emphasis on the use of such materials for applications in the broad field of biomedicine.

Complex Coacervate Phase Behavior:

Coacervation typically results in the formation of a dispersion of macromolecule-rich (*e.g.*, polymer, protein, etc.) coacervate droplets in equilibrium with a macromolecule-poor supernatant.[1,2,4,14,80,109,118-123] In addition to the high concentrations of macromolecules, the coacervate phase also retains both water and salt.[124] These droplets have the potential to coalesce over time (Figure 1) to form a bulk coacervate liquid.[1,109,118,119,121,123] Such coalescence can also be accelerated via centrifugation.[1,4,82,118,123,125] However, complexation between oppositely-charged polyelectrolytes can also result in the formation of solid precipitates and flocs. It should be noted the term “complex coacervation” has been widely applied to a large variety of materials in the literature, leading to significant ambiguity in the field.[126,127] Clear use of terminology is also complicated by the fact that it is difficult to directly observe the liquid nature (or lack thereof) of the resulting material due to the size, scale of the preparation, or hierarchical nature of the resulting assembly. While the majority of the discussion here will focus on liquid, coacervate-based materials, we will touch briefly on other, related materials.

In characterizing the self-assembly and formulation of coacervate-based materials, an understanding of coacervation phase behavior is critical. Phase behavior is one instance where differences between liquid coacervates and solid complexes is often observed, with solid materials tending to form kinetically-trapped, rather than equilibrium states. Below, we discuss the effect of various experimental parameters such as the stoichiometric charge ratio, pH, ionic strength, temperature, and the molecular-level details of the various macromolecules on coacervation.

Characterization:

Characterization of coacervation has commonly been performed using methods such as turbidimetry[1,2,4,6,7,14,15,60] and/or light scattering[16,17,29,35,111,117,128] that take advantage of the light scattered by the presence of coacervate droplets in solution. Turbidimetry, in particular, is amenable for high-throughput experiments designed to examine the effect of multiple variables such as charge stoichiometry, ionic strength, and pH on coacervate phase behavior.[1,2,4,6,7,10,11,14,15,30,37,44,60,71,74,82,109,118,119,122-124,128-157] These types of measurements are typically paired with observations via optical microscopy[1,2,62,131] to determine whether the observed phase separation is the result of liquid complex coacervation or the formation of a solid precipitate,[11,125,128,131,140,155,158-161] as well as verifying the location of observed phase boundaries. Additionally, microscopic analysis of droplet coalescence can facilitate the determination of material properties such as viscosity and surface tension (Figure 1).[91,98] In general, it is important to note that

microscopy and turbidity-style measurements tend to provide only a qualitative, phenomenological mapping of coacervate phase behavior, rather than a quantitative analysis.

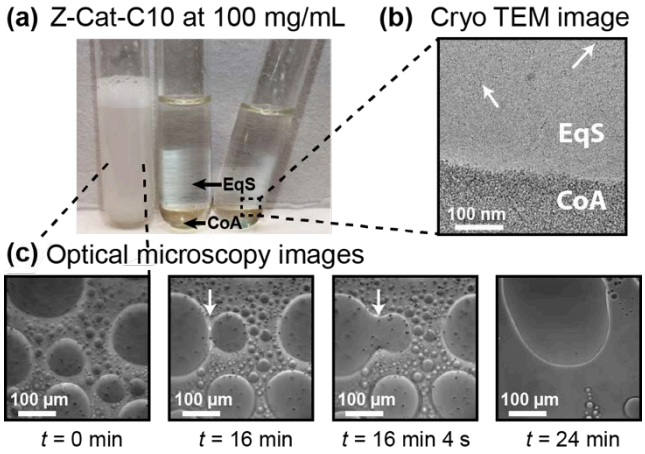

Figure 1. (a) Phase separation of 100 mg/mL Z-Cat-C10, a catechol-containing zwitterionic surfactant inspired by mussel foot protein-5 (mfp-5) in 4-mm-diameter glass test tubes. The turbid dispersions of coacervate droplets (left) and the bulk-separated phases showing the denser coalesced coacervate phase on the bottom (middle and right). The tilted tube (right) indicates the fluidity of both phases (right). **(b)** Cryo-TEM image of the interface between the dense coacervate phase (CoA) and the equilibrium solution (EqS). White arrows indicate same small aggregates found in both phases. **(c)** Optical micrographs showing the time course of the coalescence of coacervates composed of Z-Cat-C10. The 16 min, 4 s image shows coalescence of two droplets. Figure adapted with permission from Ref. [64] (Ahn, *et al.*, *Nature Commun*, (2015), *6*, 8663.).

Stoichiometry:

The charge stoichiometry, or the ratio between the number of positive and negative charges present within a formulation, is one of the most critical parameters associated with complex coacervation.[1,4,54,118-120,124,162] The ability of a mixture of materials to coacervate is directly related to the need to achieve electroneutrality within a given phase.[1,128,138,155,156] For the simple example of two oppositely-charged polymers, where both polymers have the same number of charges, electroneutrality will be achieved at a 1:1 ratio of polycation to polyanion (or a mole fraction of 0.5 for a particular species). Turbidity analysis, as in Figure 2, demonstrates that coacervation occurs in an extremely narrow range of stoichiometric compositions, centered around net neutrality. However, it is possible to broaden the observed range of compositions over which coacervation is observed through the addition of salt.[1,14,121,122] Salt enables extrinsic charge compensation of the various polyelectrolytes (*i.e.*, charge-charge pairing with a salt ion, rather than intrinsic charge compensation through an interaction with the oppositely-charged polyelectrolyte) and differential partitioning of salt vs. macro-ions between the coacervate and supernatant phases.[6,163]

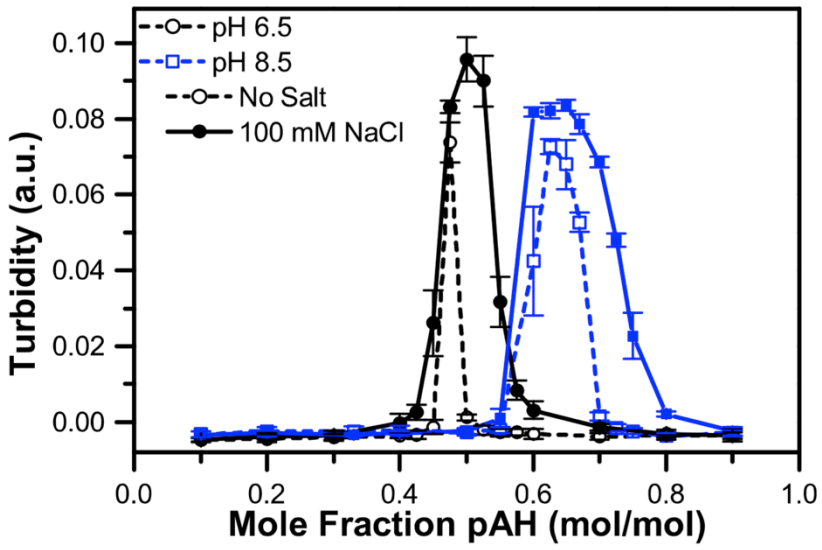

Figure 2. Turbidity plot as a function of mole fraction poly(allylamine hydrochloride) p(AH) at pH 6.5 were both (pAH) and poly(acrylic acid sodium chloride) (pAA) are fully charged (black circles) and pH 8.5 where pAH is only half charged (blue squares). Data are shown for no salt conditions (open symbols) and 100 mM NaCl (closed symbols). All samples were prepared at 1 mM total monomer concentration and complexes were prepared by adding pAA to solution containing pAH and the desired salt concentration. Figure adapted with permission from Ref. [1] (Perry *et al.*, *Polymers*, (2014), *6*, 1756-1772.).

While charge stoichiometry effects are relatively straightforward to predict for simple polyelectrolytes, where only a single type of charge group is present within a given macromolecule, intuition is much more challenging for complex molecules such as proteins, which contain both positive and negatively-charged groups. In these systems, the driving force for coacervation does not necessarily come from the overall charge of the macromolecules, but from specific charge patches on the protein surface. Thus, coacervation has been observed on the "wrong" side of the isoelectric point (pI, the point where a molecule carries no net charge) because of the dominance of local charge effects.[10,39,125,143]

Effect of pH:

While composition is one method for adjusting the charge stoichiometry of a system, pH is powerful strategy for modulating coacervation that can also be leveraged for responsive materials.[4,18,56,106,164] For weak (sometimes called annealed) polyelectrolytes, the fractional charge present on the macromolecule is a function of pH. Typical weak ionic groups include carboxylates and amines. The pH responsiveness of a single charged group can be defined by the pK_a, or the negative log of the acid dissociation constant. By definition, when the pH of a solution is equal to that of the pK_a, half of the molecules present will be charged, and half will be neutralized. It should be noted that similar definitions can be made on the basis of the base dissociation constant, pK_b. However, the two terms are mathematically interchangeable using the relationship $pK_a + pK_b \approx 14$, so for clarity we will only discuss pK_a. Thus, for acidic groups such as carboxylates, the fraction of charged groups will increase at pH values above the pK_a. However, for basic groups such as amines, the fraction of charged groups will increase at pH values below the pK_a. At solution conditions two pH units away from the pK_a, it is usually a reasonable approximation to assume that the ionic groups present are fully charged.

While the definitions of charge fraction and pH-responsive behavior are relatively straightforward for small molecule ions, polyelectrolytes are more complicated to describe. The challenge in describing the effects of pH on a charged macromolecule lies in the fact that no single pK_a value can be used to describe the entire molecule, and that the "apparent pK_a" changes as a function of the number of charged groups. Thus, it is more accurate to discuss the degree of ionization (α) for a simple polyelectrolyte, although pK_a values have been more commonly reported. A particular challenge in using pK_a as a simplified method for describing the charge state of a polyelectrolyte is the fact that the degree of ionization can be a strong function of salt concentration, sometimes shifting the "apparent pK_a" several pH units.[165]

The effect of pH on the stoichiometry of complex coacervation can clearly be observed in Figure 2. For the system of poly(acrylic acid sodium salt) (pAA) and poly(allylamine hydrochloride) (pAH), both of which are weak polyelectrolytes, pH = 6.5 represents a solution condition that is both two pH units away from the apparent pK_a of both polyelectrolytes, and equidistant between the two apparent pK_a values.[1] Thus, it is reasonable to assume that both polymers are equally charged. This assumption is further confirmed by the sharp peak in turbidity observed at a 1:1 mole ratio (mole fraction pAH = 0.5). However, at a solution pH = 8.5, corresponding to the apparent pK_a for pAH, the peak in turbidity shifts to a mole ratio of 2:1 pAH:pAA (mole fraction pAH = 0.67), as would be expected for conditions where the pAH is only half charged. Similar shifts in stoichiometry are also observed when multiple polyelectrolytes are present, with coacervation favoring conditions of net neutrality.[118]

As mentioned above, predicting the coacervation behavior for complex polyelectrolytes, such as proteins that contain multiple charged species, is much more challenging. The isoelectric point (pI) is a common parameter used to describe the point at which a protein has no net charge. When the pH is below the pI, a protein carries a net positive charge, whereas it is net negative when the pH is above its pI. However, this type of general parameter is unable to describe the presence (or absence) of local charge patches, which may dominate the complexation interaction.[10,39,125,143] Thus, understanding the effect of environmental pH on the formation or dissolution of protein-containing coacervates is a non-trivial undertaking. However, pH can be a powerful strategy in designing responsive materials for sensing and/or the triggered release of therapeutics.[4,84,106,114,166]

Effect of Salt:

Another environmental factor that heavily impacts the formation and dissociation of coacervates is the ionic strength.[1,6,74,147,159,164] At low concentrations, the presence of salt can facilitate coacervation by modulating the strength of the electrostatic interactions between polyelectrolytes and enabling extrinsic charge compensation to allow for molecular rearrangement.[1,6,163] In fact, a transition from solid precipitate to liquid coacervate has been observed as a function of salt for some systems.[6,120,121] However, at high enough ionic strength, the concentration of salt present in the system disfavors the entropic release of bound counterions, inhibiting coacervate formation. Turbidimetry allows for observation of these trends, though we caution against interpreting the details of such curves too finely, due to the qualitative limitations of turbidity measurements (Figure 3).[1,109,118-122,167]

The most telling and accurate result from a turbidimetric salt experiment is identification of the critical salt concentration, or the point at which phase separation is no longer observed.[1,118-122] To a first approximation, trends in the critical salt concentration scale directly with ionic strength;

however, there are important secondary effects. As can be seen in Figures 3a and 3b, the divalent salts $CaCl_2$ and Na_2SO_4 result in a dramatically lower critical salt concentration than monovalent NaCl. Interestingly, a much more significant decrease in the critical salt concentration was observed for the divalent cation Ca^{2+}, than for the divalent anion SO_4^{2-}. This difference was explained in several related ways, including differences in the "hardness" of the various ions, the free energies of hydration, and also the chaotropic and kosmotropic Hofmeister behavior of the ions.[1,168-174] Similar, though more subtle behavior can also be observed upon examination of additional ions, such as a halide series of sodium salts (Figure 3c) or other ionic functionalities (Figure 3d). As with pH, the tunable dependence of coacervation on salt concentration can be harnessed to control the responsiveness of a material, including sensing, encapsulation, and release.[74,147,159,164]

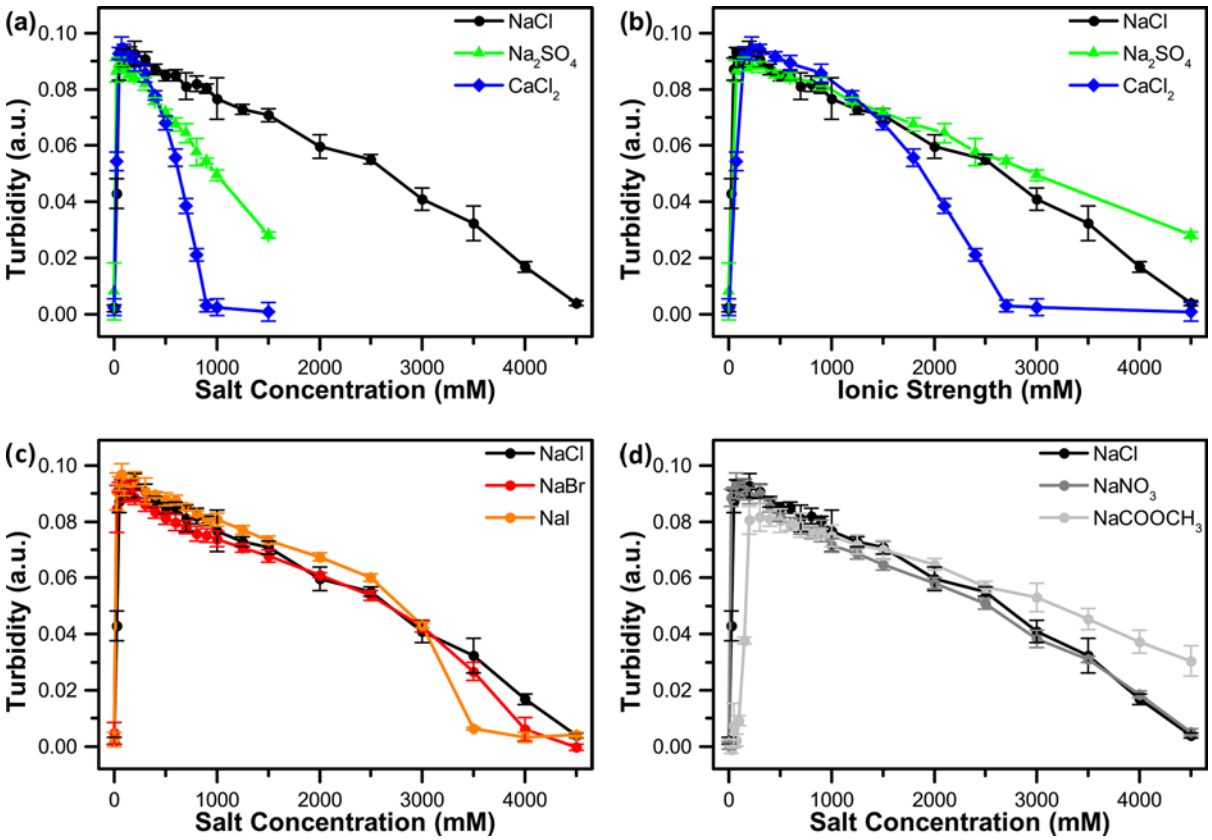

Figure 3. Plots of turbidity showing a comparison of **(a)** a series of mono and divalent salts. **(b)** A plot of turbidity vs. ionic strength for the salts shown in **(a)**. Additional comparisons of a series of **(c)** a series of sodium halide salts and **(d)** other monovalent sodium salts. All samples were prepared at 1 mM total monomer concentration, 50/50 mol% pAA/pAH ratio at pH 6.5 and complexes were prepared by adding pAA to solution containing pAH and the desired salt concentration. Figure adapted with permission from Ref. [1] (Perry *et al.*, *Polymers*, (2014), *6*, 1756-1772.).

Effect of Temperature:

In general, coacervation between oppositely-charged polymers tends to show a relatively weak temperature dependence. For instance, isothermal titration calorimetry (ITC) studies of polypeptide-based coacervates detected only small changes in both the enthalpy and entropy of coacervation as a function of temperature.[123] It should be noted that there are a variety of examples where a stronger temperature effect has been reported; however, much of this temperature dependence correlates with the behavior of the individual molecules, such as proteins or surfactants, rather than the coacervation-driven self-assembly.[10,11,175-178]

Thermodynamic Phase Diagrams:

While the qualitative nature of turbidity and/or light scattering experiments typically provides only a phenomenological characterization of coacervation, quantitative parameters such as the critical salt concentration can be extracted from such data to map out thermodynamic phase behavior. One of the major limitations of turbidity-style measurements is inability to correlate phenomenological observations of coacervate formation with compositional information. However, at the critical salt concentration, where phase separation is no longer observed, one can reasonably take the composition of the very last miniscule droplet of coacervate phase to equal that of the overall sample – defining a single point on the binodal curve. It is unfortunate, however, that very few thermodynamic phase diagrams have been reported, despite the availability of a large body of work on the phenomenological characterization of coacervation in the literature.

A schematic depiction of a series of binodal curves for a polymer-based coacervate system is shown in Figure 4. The location of the phase boundaries are indicated on a plot of salt concentration vs. polymer concentration, for a given stoichiometric composition, pH, temperature, etc. The two-phase region where coacervation is observed is located underneath the binodal curve, while the single-phase region is located above the curve. Samples prepared at a composition falling within the two-phase region will undergo coacervation and form a polymer-rich coacervate phase and a polymer-poor supernatant phase, the equilibrium compositions of these two phases are defined by a tie-line. In Figure 4, the tie-line indicates that the concentration of salt in the supernatant is higher than that in the coacervate, as suggested by recent theoretical predictions for coacervate phase behavior,[179] however many studies use the simplifying assumption that the salt concentration is the same in the two phases.[133,162] Parameters such as polymer chain length can increase the width of the two-phase region, to an asymptotic limit of infinite chain length. Polymers with a higher charge density will similarly increase with width of the two-phase region.[162,179] Finally, the top-most point on the binodal curve, known as the critical point (where spinodal decomposition occurs), asymptotically approaches a finite limit in salt concentration at zero polymer concentration with increasing polymer chain length.[179] Thus, for a given polymer system, there is an absolute limit on the range of ionic strengths over which coacervation can be observed.

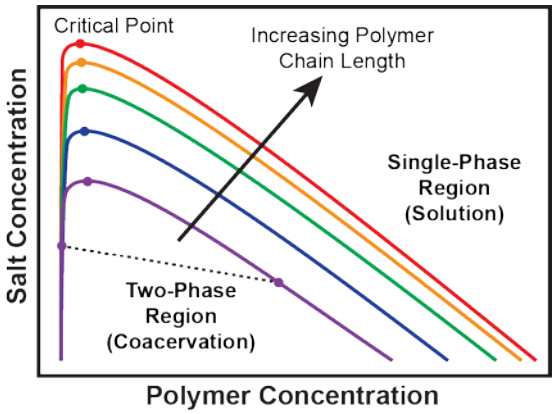

Figure 4. Schematic representation of a series of thermodynamic phase diagrams, or binodal curves, as a function of salt concentration and polymer concentration (for a given stoichiometry, solution pH, and temperature), defining the boundary between the two-phase region of coacervation (beneath the curve) and the single-phase solution region (above the curve). The critical point is indicated at the highest point of each curve. The dashed tie line defines the equilibrium concentration for a coexisting coacervate and supernatant phase. Increasing polymer chain length can drive an increase in the width of the two-phase region, as indicated by the arrow. Similar trends have been observed for increasing polymer charge density.

Kinetically Trapped Materials and Precipitation

As with the liquid-liquid phase separation that drives complex coacervation, variations in the charge stoichiometry, ionic strength, and pH of the solution can also have a significant impact on the formation of solid precipitates or flocs. Variations in these parameters can lead to transitions from a single solution phase to solid precipitates, liquid coacervates, and then back to a single phase.[44,125,158,159,161] However, the solid nature of these materials means that it is challenging to access the lowest thermodynamic state, and thus solid materials often suffer from kinetic trapping that can alter their phase behavior, responsiveness, and material properties. One of the most commonly reported observations suggesting kinetic limitations in sample preparation for both precipitates and coacervates is a different response related to the order in which the various components of the mixture are added. While careful experimental design and equilibration time can help to minimize these effects in coacervates, because of their liquid nature, kinetic trapping is much more difficult to overcome for solid materials.

Molecular Design:

In addition to external solution variables, the molecular characteristics of the component materials also play important roles in defining the extent of coacervation and the resultant materials properties.

Chirality:

An intriguing variable affecting the coacervation of polypeptides is chirality. Naturally-occurring proteins are composed almost entirely of *L* amino acids. Thus, in attempting to use charged polypeptides such as poly(lysine) and poly(glutamate) as protein mimetic polymers, it would be reasonable to attempt complexation with enantio-pure polymers composed entirely of *L* amino acids. However, a recent study demonstrated that in order for complexation to result in liquid-liquid phase separation, it was necessary for at least one of the polypeptides to be composed of a racemic, or 50/50 mixture of *D* and *L* monomers (Figure 5a), otherwise a solid precipitate with strong β-sheet character results.[14] These β-sheet precipitates could be disrupted and "melted" to form an apparent liquid coacervate with the addition of urea. The importance of hydrogen bonding was further highlighted through a comparison of the critical salt concentration for coacervates composed of a single racemic polypeptide and coacervates composed entirely of racemic polypeptides. A significantly higher critical salt concentration was observed when only a single racemic species was present, suggesting that hydrogen bonding could be used as an additional variable to control the salt-responsiveness of a coacervate-based material.

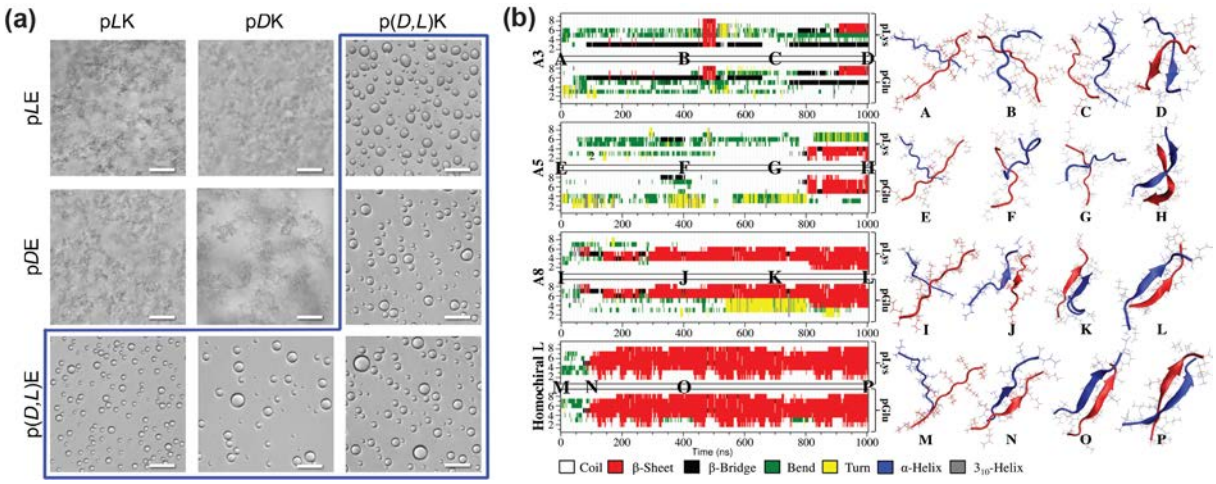

Figure 5. (a) Bright-field optical micrographs showing the liquid coacervates or solid precipitates resulting from the stoichiometric electrostatic complexation of *L*, *D*, or racemic (*D,L*) poly(lysine) (single letter abbreviation K) with *L*, *D* or racemic (*D,L*) poly(glutamate) (single letter abbreviation E) at a total residue concentration of 6 and 100 mM NaCl, pH 7.0. Complexes are formed from p*L*K + p*L*E, p*D*K + p*L*E, p(*D,L*)K + p*L*E, p*L*K + p*D*E, p*D*K + p*D*E, p(*D,L*)K + p*D*E, p*L*K + p(*D,L*)E, p*D*K + p(*D,L*)E, p(*D,L*)K + p(*D,L*)E. Liquid coacervate droplets are only observed during complexation involving a racemic polymer. Scale bars are 25 μm. Figure adapted with permission from Ref. [14] (Perry *et al.*, *Nature Commun*, (2015), *6*, 6052.). **(b)** Secondary structure of each residue vs. time for various 1 μs MD simulations of 10-amino acid polypeptide pairs. "A" denotes simulations containing non-homochiral peptides of poly(glutamate) (PGlu, blue), with a specified number of continuous *L* amino acids in the center of the chain, in complex with a homochiral poly(*L*-lysine) (PLys, red). The structures of PLys and PGlu are shown at 0, 400, 700, and 1000 ns for each pair. Figure adapted from Ref. [13] (Hoffmann *et al.*, *Soft Matter*, (2015), *11*, 1525-1538.) with permission from The Royal Society of Chemistry.

The molecular-level details describing this chirality-driven phenomenon were further elucidated through the use of molecular dynamics (MD) simulations.[13,14,126] These 1 μs simulations, coupled with supporting Fourier transform infrared spectroscopy (FTIR) data confirmed that formation of β-sheet structured precipitates was the result of backbone hydrogen bond formation between interacting pairs of oppositely-charged polypeptides. Hydrogen bonding between peptides eliminated sites for peptide-water hydrogen bonds, helping to expel water from the resulting complex. In contrast, the combination of *D* and *L* of amino acids present in a racemic polypeptide disrupted the ability of the system to form hydrogen bonds due to steric effects.

One interesting feature of the MD results for the coacervate-forming system of poly(*L*-lysine) with poly(*D,L*-glutamate) was the appearance of transient areas of β-sheet structure. To answer the question of how many continuous amino acids of the same chirality were needed to stabilize the formation of a stable β-sheet structure, additional MD simulations were performed.[13] The data, summarized in Figure 5b suggest that a stable β-sheet requires the presence of eight continuous amino acids of the same chirality. This result suggests the potential for using sequence control of amino acid chirality as a means for modulating the number of hydrogen bonding interactions present in a polypeptide-based material, and thus the resultant material properties.

It should be noted that the potential for hydrogen bond-driven precipitation is only a concern for polypeptides or protein-based materials where stable secondary structure is not already present. Thus, for stable α-helical peptides or folded proteins, the internal hydrogen bonds associated with the secondary structure of the material are not accessible.[2,4,16-18,71,73,74,147] However, these studies are interesting in the context of naturally-occurring liquid granules observed in cells, where the phase separation is commonly associated with interactions between RNA and intrinsically disordered proteins that lack any stable secondary structure. Thus, an open question in the field of polypeptide-based coacervation is how the role of chemical sequence affects the ability of a particular system to undergo coacervation, as well as the resultant material properties.[7,88-100,102-105]

Branching and Molecular Topology:

Another architectural feature of both natural and synthetic polymers is the presence of branches, loops or other types of molecular topology. While reports on coacervation include variety of branched polymers, the majority of efforts have utilized naturally occurring polymers that are not well defined either chemically or physically.[19,158,180-183] However, advances in polymer chemistry have enabled the synthesis of increasingly dense branched and brush polymer structures. These chemistries represent an intriguing opportunity to explore the steric limitations of electrostatic interactions.

Looking beyond simple branching, recent work modeling the distribution of counterions on polyelectrolytes of different architectures has demonstrated the critical role of molecular topology.[184] Extension of this work into the field of coacervation could provide some interesting results into the role of the entropic driving force of counter-ion release, and how this can be modulated by molecular design.

Hierarchical Structure:

Looking beyond molecular topology, hierarchically-structured coacervate-based materials have also been reported. While coacervation of homopolymers enables bulk phase separation (Figure 6a),[1,2,4,13,14] coupling a polyelectrolyte domain to a hydrophobic polymer block drives the formation of nanometer-scale micelles with a coacervate corona (Figure 6b).[185] Alternatively, coupling the polyelectrolyte domain to a neutral, water-soluble polymer such as poly(ethylene glycol) (PEG) creates a molecular interface that drives microphase separation and the formation of coacervate-core micelles (Figure 6c).[49,50,52,53] Modulation of the length of the neutral and polyelectrolyte blocks has also been reported to lead to coacervate-core vesicles (Figure 6d).[73,85,186] Extension of this strategy to a triblock copolymer system enables the formation of flower-like micelles under dilute conditions, or structured, hydrogel-like coacervate-based materials at higher concentrations, where the coacervate domains act as crosslinking points within the network (Figures 6e and 6f).[48-51,55,187,188] More complex coacervate-based geometries analogous to structures observed in traditional solvophobic block copolymers (*i.e.*, bicontinuous, gyroid, etc.) should also be possible.

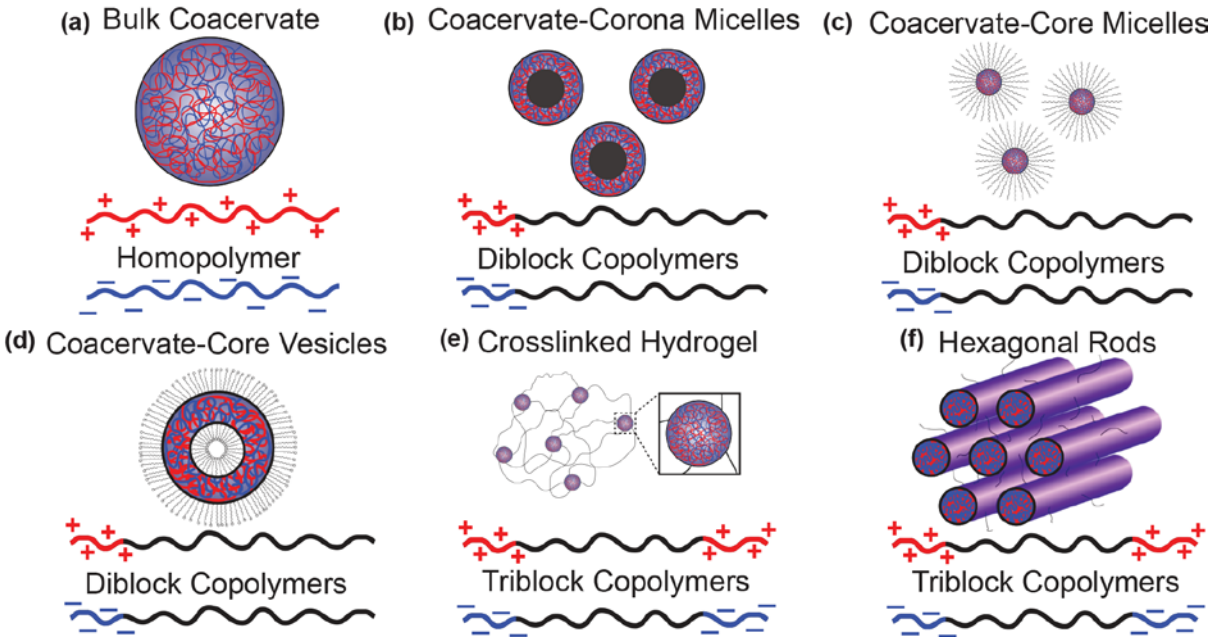

Figure 6. Architectural schemes of various hierarchically-structured coacervate-based materials including **(a)** bulk coacervates, **(b)** coacervate-corona micelles, **(c)** coacervate-core micelles, **(d)** coacervate-core vesicles (also known as polyion complex vesicles, or PICsomes), and triblock copolymer coacervate hydrogels with both **(e)** spherical and **(f)** hexagonal coacervate geometries.

While details of the various architectures have significant implications for the material properties and utility of the various coacervate-based materials, the effects of charge stoichiometry, pH, and ionic strength are consistent between bulk and micro-phase separated coacervate-based materials.[35,37,38,48-51,132,148,151,185] Similarly, the observed trends relating to polypeptide chirality are transferrable to microphase-separated systems.[14] However, the length-scales associated with the

micro-phase separated nature of these materials makes direct confirmation of the liquid or solid nature of the resulting coacervate domains extremely challenging. Perhaps the best evidence for the "liquid" nature of such materials is related to the fast equilibration time and monodispersity of coacervate-core micelles, as compared with parallel micellar materials that would be expected to form more solid-like core structures.[14,37,186,189,190]

It is important to note that the geometric constraints of microphase separation do impose additional considerations on the self-assembly of the system. As mentioned above, the balance between the length of the polyelectrolyte block and the neutral polymer block controls the geometry of the system (*i.e.*, micelles[34,37,38,132,148] vs. vesicles[73,85,186]). Furthermore, micellar systems typically contain a well-defined number of molecules, or a characteristic aggregation number. Research has also shown that for coacervate-core micelles, where both of the polyelectrolytes are present as block copolymers, the geometric constraints of the system enable chain-length recognition, such that complexation is only favorable between block copolymer of the same length charge block.[132]

Applications:

Complex coacervate-based materials have been used for a variety of applications across a range of disciplines, including nutraceutical and drug delivery platforms, sensors, biomimetic adhesives, and cartilage mimics. In the following sections, we survey the use of coacervate-based materials across the broad field of biomedicine.

Encapsulation:

One of the most significant areas for complex coacervation has been as a method for encapsulation.[2,4,7,8,16-18,33,35,36,38,72,73,110,117,180,191] Coacervation-based encapsulation has been widely used in food science, medicine, sensing, and in the development of nanoreactors.[19,27,57,59,77,107,108,110,114,115,192-199] Encapsulation can be achieved by utilizing the cargo material as part of the coacervate matrix,[4,8,15,72,81,128,136,137,140,146,200-203] as a result of specific interactions,[115] or by preferential partitioning.[4,17,18,29,72,74,87] In all of these cases, two major advantages of coacervation are (i) the ability to perform encapsulation in a purely aqueous environment,[3,4,73,106,190,204] and (ii) the potential for dramatically enriching the molecule of interest in the macromolecule-rich coacervate phase, as compared to the original solution.

The encapsulation of proteins within a coacervate phase can represent a particular challenge due to the fact that not all proteins of interest are strongly charged. A strategy for overcoming this limitation was recently reported for the case of binary, protein-polyelectrolyte coacervates. In this work, the natural charge state of various proteins was supplemented through the use of conjugation chemistry to create artificially supercharged proteins using succinic anhydride.[15] Furthermore, the authors were also able to elegantly demonstrate that the degree of supercharging necessary to effect coacervation (as defined by the ratio of the number of negative to positive charged groups, for subsequent coacervation with a polycation) is relatively low – on the order of 1.1 to 1.4 (Figure 7a).

Ternary systems of coacervates have also been reported as an effective strategy for encapsulating proteins.[4,72] Rather than relying on the charge of the protein itself to drive coacervation, the use of a ternary system of proteins and polymers allows for the initial formation of an intermediate complex between the protein of interest and an oppositely-charged polyelectrolyte, the overall charge of which is dominated by the polyelectrolyte. Coacervation is then induced by the addition of a second

polyelectrolyte, which interacts directly with the intermediate complex (Figure 7b).[4] While a broad exploration of ternary composition space has not been performed, preliminary reports suggest a trade-off between encapsulation efficiency and total protein loading, as would be expected given the need to maintain charge neutrality in the coacervate phase. Further exploration of ternary composition space represents an exciting area for further investigations.

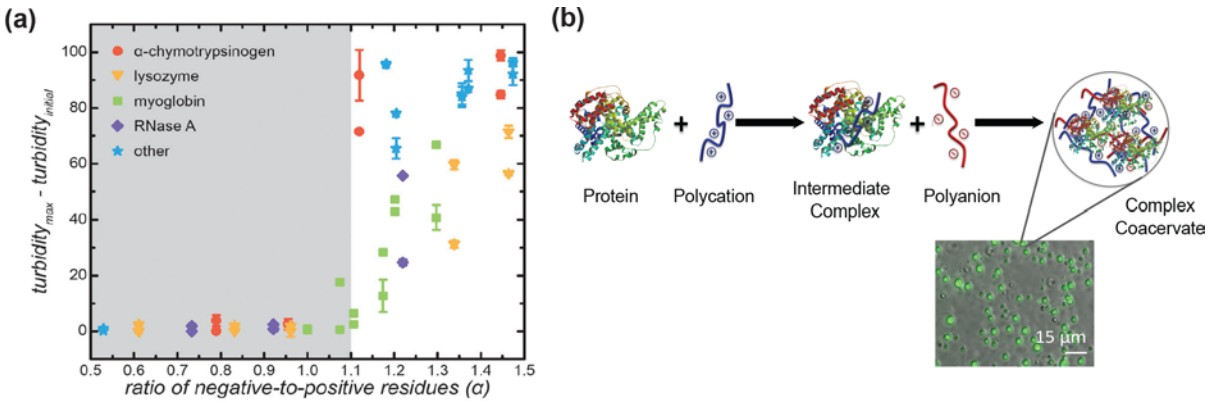

Figure 7. (a) Plot of changes in turbidity as a function of the ratio of negative-to-positive residues on the protein. The grey shaded region corresponds to proteins that do not undergo phase separation. Figure adapted with permission from Ref. [15]. (Obermeyer *et al.*, *Soft Matter*, (2016), *12*, 3570-3581.) **(b)** Encapsulation of bovine serum albumin (BSA) into a coacervate. Positively-charged poly(*L*-lysine) (PLys) is added to the negatively-charged protein to form an intermediate complex. Negatively-charged poly(*D,L*-glutamate) (PGlu) is then added to form the complex coacervate. Figure adapted with permission from Ref. [4] (Black *et al.*, *ACS Macro Lett*, (2014), *3*, 1088-1091.).

Upon encapsulation, it is critical to test whether the coacervation process adversely affected the guest molecules. This consideration is particularly important for proteins, as opposed to small molecules, and can be assayed using spectroscopic methods such as circular dichroism (CD) and FTIR, which are sensitive to the protein secondary structure. Fortunately, coacervation is a relatively gentle method for encapsulation that maintains proteins in an aqueous environment. Typical reports have shown minimal evidence for adverse effects of coacervation on protein structure.[4,16,205]

Beyond the prospect of coacervation serving as a gentle method of encapsulating proteins, there is also significant potential for coacervation to enhance the stability of guest biomacromolecules. The dense, macromolecule-rich coacervate phase can provide entropic stabilization, based on crowding and excluded volume effects that disfavor protein unfolding and denaturation, as well as enthalpic stabilization based on interactions between the coacervate matrix and the guest molecules.[2,4,7,31-33,71,117,206-208] Such stabilization has also been shown to improve the thermal stability of proteins, and reduce their degradation over time.[3,31] For example, an increase in the melting temperature and resistance to denaturation by urea was reported for trypsin upon incorporation into coacervates of cross-linked poly(ethylene glycol)-*block*-poly(α,β-aspartic acid) (PEG-PAA).[31] This increase in the overall stability of the protein resulted in an improvement in the ability to store trypsin formulations over time – a key issue for therapeutics and other biomaterials during transportation and storage. Similar strategies have long been utilized for the delivery of DNA and RNA to cells to protect against nuclease degradation.[80]

Delivery Platforms:

Building on the strengths of complex coacervation for encapsulation, such materials have been commonly used as a platform for the delivery of nutraceuticals,[194-196,198,199] drugs,[34,77,209] proteins,[4,8,16-18,29,32,34,71-75] RNA,[7,81,82] and DNA.[28,34,79,80,210] The lack of organic solvents in coacervation

has added benefits in the context of drug delivery, beyond those related to the gentle encapsulation of biomolecules. Biocompatibility is a critical design aspect for formulations intended for use *in vivo*, and a fully aqueous processing scheme eliminates the need for additional steps to eliminate even trace amounts of organic solvents. This biocompatibility can be further achieved through the use of naturally-derived biomacromolecules,[4,16,73,107,108] although a wide range of safe and effective synthetic polymers have also been reported.[4,73,109,110]

Drug delivery platforms typically address multiple challenges, including (i) protection and/or isolation of the cargo, (ii) enabling targeted delivery and uptake into the cells or tissues of interest, and (iii) controlled release of therapeutics over time. A variety of reports have demonstrated the efficacy of coacervation as the basis of a drug delivery platform, taking advantage of the flexible and modular capabilities of charge-driven self-assembly to address each of these challenges.

The motivation driving cargo encapsulation is typically different for small molecule therapeutics compared to biomacromolecules.[34,209,211] Small molecule drugs tend to suffer from poor solubility in water, thus requiring specialized encapsulation to facilitate delivery at therapeutically-relevant concentrations.[43,212] While similar solubility obstacles can exist for proteins and other biomolecule-based therapeutics, maintaining the stability of the sample and avoiding degradation from proteases and nucleases during delivery is typically a more significant challenge. A variety of reports have demonstrated the protective capacity of coacervate-based materials, including bulk coacervates,[76,200-202] coacervate-core micelles,[34,81] and coacervate-core vesicles (also known as polyion complex vesicles, or PICsomes).[186]

From a delivery standpoint, bulk and hydrogel-like coacervate-based materials are typically the most useful in circumstances that allow for bolus-style delivery (*i.e.*, direct application or injection of the material to the site of interest). For example, coacervate-based hydrogels composed of alginate and chitosan were shown to enhance the proliferation of cells *in vitro* while accelerating healing efficiency and wound closure in a rat model.[213] In another series of reports, the cationic polymer poly(ethylene argininylaspartate diglyceride) (PEAD) was used in concert with the glycosaminoglycan heparin to form coacervate-based delivery vehicles that take advantage of the strong binding affinity between heparin and various growth factors to enable cargo encapsulation and protection. Applications included the use of heparin-binding epidermal growth factor-like growth factor (HB-EGF) to accelerate wound healing,[197] fibroblast growth factor-2 (FGF2) to enhance angiogenesis in both surface wounds and after myocardial infarction (Figure 8a),[76,78] stromal cell-derived factor (SDF)-1a for vascular regeneration,[108] bone morphogenetic protein-2 for stem cell differentiation and bone formation,[214] nerve growth factor (NGF) for nerve regeneration,[110] and the anti-inflammatory cytokine interleukin-10 (IL-10).[215]

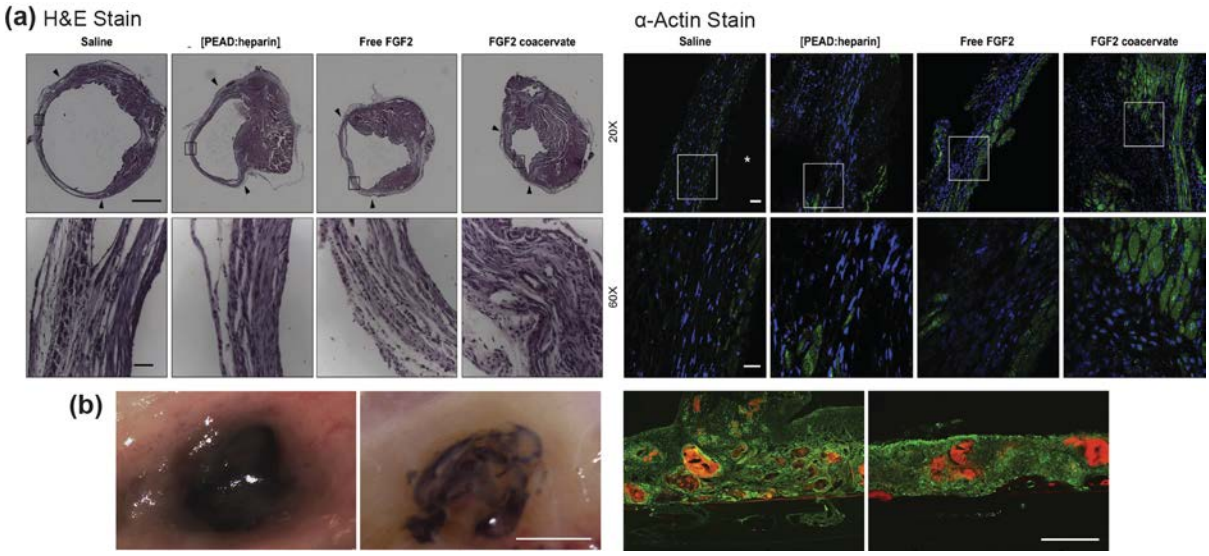

Figure 8. (a) Comparison of H&E (scale bar is 1 mm) and α-actinin (scale bar is 50 μm) stained tissues for infarcted myocardium receiving treatments of saline, [PEAD:Heparin], free FGF2 and FGF2 coacervate. Application of the coacervate FGF2 formulation significantly reduced the infarct area, preventing ventricular dilation and preserving cardiac fibers, compared with the other treatment strategies. α-actinin stained tissues demonstrate enhanced preservation of cardiomyocites in the infarct zone for the FGF2 coacervate treatment. Figure adapted with permission from Ref. [78]. (Chu *et al.*, *Biomaterials*, (2013), *34*, 1747-1756.) **(b)** Adhesive complex coacervate adhesive analysis on skull surface (left) and CD68 immunoreactivity (green) associated with adhesive (red). Scale bars represent 500 μm. Figure adapted with permission from Ref. [57] (Winslow *et al.*, *Biomaterials*, (2010), *31*, 9373-9381.).

The issue of cargo protection is often coupled with strategies to facilitate cellular uptake. For instance, the vast majority of non-viral strategies for gene delivery rely on electrostatic complex formation between the negatively-charged DNA or RNA and a positively-charged carrier polymer, surfactant, or lipid.[216-219] Such complexation helps to protect against attack from nucleases.[220,221] The positively-charged carrier materials also help to facilitate cellular uptake by masking the negative charge of the DNA or RNA[222] and facilitating an attractive interaction with the negatively-charged cellular membrane.[223] Reports of coacervate-based platforms for gene delivery include both bulk complexes[200-203] and micellar[38,81,220,221,224-226] systems for the delivery of plasmid DNA, microRNA,[81] and siRNA[226] (small interfering RNA). Specific diseases targeted by these approaches include atherosclerosis[81] and cancer.[226]

While encapsulation can protect cargo molecules during administration, two critical aspects of targeted delivery are the need to direct the therapeutic to a specific area of interest, followed by triggered release. Targeted delivery can increase the efficiency of a therapeutic dose while decreasing the potential for adverse side effects resulting from systemic exposure. The modular nature of coacervation allows for the straightforward incorporation of specific targeting moieties.[77,81,181] For instance, the efficacy of two different peptides incorporated onto the corona of coacervate-core micelles has been reported for the targeted delivery of microRNA to treat atherosclerosis.[81]

The triggered release of therapeutic cargo can be achieved through a variety of means including changes in pH, ionic strength, or specific degradation events (*i.e.* proteolysis). The choice of release mechanism is often specific to a particular application. However, for many biomedical applications, changes in pH associated with cellular uptake via endocytosis can be used to trigger disassembly of

the coacervate-based delivery vehicle. Alternatively, more stable interactions can be utilized for controlled release systems.[16,19,76,77,106,107,110]

While the idea of targeted delivery is typically associated with medical applications, food scientists have recently begun to adapt older concepts where complex coacervation has been used to entrap flavors and oils for the delivery of proteins, nutraceuticals, and other water-soluble actives.[194-196] Just as delivery platforms in biomedicine can be harnessed to facilitate uptake, materials design strategies are being utilized to enable more efficient absorption of nutrients, vitamins, and antioxidant molecules during digestion.[198,199] Here, the design parameters are limited in terms of biocompatibility, the availability of bulk quantities of food-grade, cost, and the need to generate a delicious product.

Bioinspired Adhesives:

Just as aqueous processing enabled encapsulation and delivery applications, the aqueous liquid-liquid phase separation aspect of complex coacervation has driven significant advances in the area of bioadhesives.[9,56-70,227,228] Coacervate-based adhesives were first observed in natural systems, such as the sandcastle worm and mussels.[58,62,64,65,229] The sandcastle worm builds a tube-like dwelling by mixing together oppositely charged proteins, forming a complex coacervate phase that it uses to glue together individual grains of sand.[230] Similarly, mussels secrete a series of mussel foot proteins (mfp), which form the basis of a coacervate-based adhesive. The challenge in these living systems, as well as many biomedical applications is the need to create an effective adhesive that is capable of working in a wet environment.

The two main challenges in developing an underwater adhesive are (i) avoiding dilution and (ii) accessing the surfaces of interest to establish an adhesive interaction. The use of coacervate-based materials circumvents the issue of dilution by taking advantage of the liquid-liquid phase separation to create a macromolecule-rich adhesive material. In the case of marine animals, it is also necessary for this coacervate to be stable at the ionic strength of seawater. Furthermore, coacervates typically have an extremely low surface tension with water (~1 mJ/m^2).[109,152] This low surface tension facilitates spreading of the coacervate phase on surfaces and penetration into tight cracks etc. However, to achieve adhesion, it is necessary to displace surface-bound water. A recent study inspired by the chemistry of mussel adhesives showed that neighboring lysine and catechol moieties (*i.e.*, dopamine, DOPA) in these natural adhesives interacted synergistically to prime the surface for adhesion. The alkyl amine group from the lysine was able to penetrate the hydrated cation layer present on a mica surface, allowing the bidentate catechol group to form adhesive hydrogen bonds.[231] The adhesive can then be cured by a subsequent pH change to form a load-bearing solid.[65]

The main biomedical areas for such adhesives include bone,[56,57] cartilage,[232,233] and tissue repair,[56,58,230,233-237] as well as implants.[9] For example, coacervate-based adhesives composed of poly(acrylamide-co-aminopropyl methacrylamide)-poly(ethylene glycol diacrylate) and poly(2-(methacryloyoxy)ethyl phosphate dopamine methacrylamide)-poly(ethylene glycol diacrylate) were used *in vitro* to seal an iatrogenic defect in a fetal membrane patch. The adhesives were able to function, as well as withstand traction and turbulence without leakage of fluid or slippage.[59] Cytotoxicity tests revealed the adhesive to be non-toxic and may help prevent iatrogenic preterm premature rupture of the membranes.[59] In another example, craniofacial reconstruction via a non-cytotoxic coacervate adhesive of gelatin and phosphodopamine in rats was conducted (Figure 8c).[57]

The adhesive was used to attach a piece of circular bone in the skull and, after recovery from anaesthesia, were allowed to move freely. The adhesive was observed to effectively hold the bone in place despite free movement of the animals. Furthermore, as the adhesive material was resorbed by the body, it was replaced by new bone without affecting alignment.[57] Though these and other examples have demonstrated the potential for coacervate-based adhesives, further *in vivo* testing and ultimately clinical experiments are still needed to fully validate their safety and efficacy.[233] However, one particular advantage of bio-inspired coacervate-based adhesives would be the potential for repairing tissue and bone without the need to remove the adhesive at a later time.

Protocells and Membraneless Organelles:

Historically, one particularly contentious topic surrounding complex coacervation was the potential for these phase-separated compartments to serve as a type of protocell that could form the basis for the evolution of life.[7,30,238-245] This hypothesis, originally put forth by Oparin,[156,240,245-248] has re-emerged in the scientific literature though there are contentious discussions about the functional practicality of such membraneless compartments,[88,91,95,249] particularly with respect to their ability to sequester materials such as RNA without exchange. However, such systems do allow for the formation of model protocell environments that allow for the testing of specific aspects of biogenesis. In a recent report, reversible compartmentalization was demonstrated as a result of coacervation between RNA and a cationic peptide (Figure 10a).[7,82,250] This system represented a minimal synthetic model demonstrating the regulation of droplet formation based on changes in the peptide phosphorylation state using a kinase/phosphatase enzyme pair.

Beyond the historical debate, phase-separated and coacervate-like materials have been increasingly discussed in the context of cellular compartmentalization. Improvements in microscopy and labelling strategies has led to the discovery of a tremendous range of membraneless cellular compartments that harness liquid-liquid phase separation to drive functionality. Such compartmentalization has been typically associated with interactions between intrinsically disordered proteins (IDPs) and oligonucleotides. The formation of stress granules has been observed as a mechanism for cells to arrest certain metabolic pathways while retaining the enzymatic machinery for later use.[251] Granule formation has also been associated with loci of transcription[93,98,252-254] and ribosome biogenesis, such as nucleoli (Figure 9a,b).[127,253] Compartmentalization also enables passive noise filtration, which can further help to increase the predictability of transcriptional outputs.[254]

In addition to the potential benefits of compartmentalization, aberrant phase transitions have also been correlated with disease states. FUS is a prion like IDP associated with the neurodegenerative disease ALS that has been shown to form liquid compartments as a result of stress and/or DNA damage. However, aging experiments demonstrated that mutations in FUS associated ALS resulted in an accelerated liquid-to-solid transition (Figure 9c).[104] While it should be noted that complex coacervation is not the driving force behind the formation of all membraneless organelles,[127] there is tremendous potential for parallel scientific exploration in the space between pure biology and pure materials science.

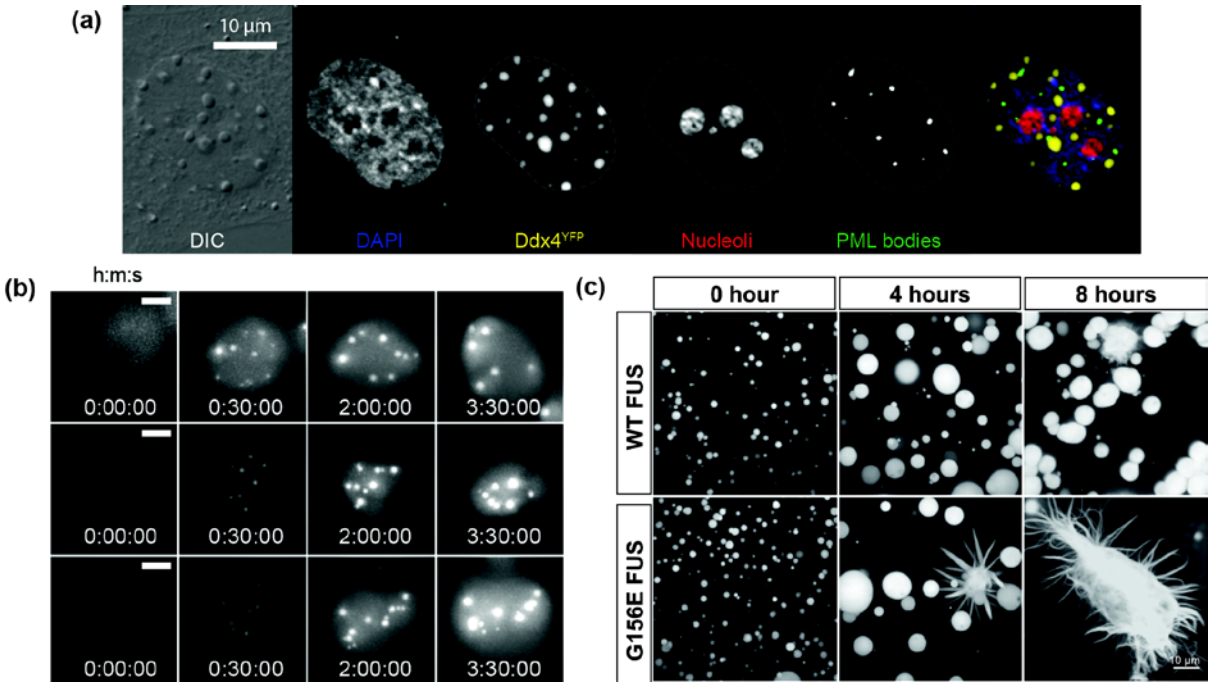

Figure 9. (a) Differential interface contrast (DIC) and fluorescence micrographs of a HeLa cell expressing Ddx4^{YFP}. Ddx4^{YFP} forms dense, spherical organelles in the nucleus. Cells were stained with antibodies to visualize nucleoli, PML bodies, nuclear speckles, and Cajal bodies. Figure adapted with permission from Ref. [253]. (Nott *et al.*, *Mol. Cell,* (2015), *57*, 936-947.) **(b)** Time-lapse imaging of a nuclear body assembly in transiently transfected HeLa cells expressing Nephrin intracellular domain (NCID). Scale bar represents 5 µm. Figure adapted with permission from Ref. [127]. (Pak *et al.*, *Mol. Cell*, (2016), *63*, 72-85.) **(c)** Representative images of the morphological changes in *in vitro* droplets of wild-type (WT) and G156E FUS during an "aging" experiment over 8 hr. Figure adapted with permission from Ref. [104]. (Patel *et al.*, *Cell*, (2015), *162*, 1066-1077).

Nano / Bioreactors:

The compartmentalization afforded by coacervation can also be harnessed to define micro- or nanoscale reaction chambers. Coacervate droplets and coacervate-core micelles have been used to entrap enzymes to create nanoreactors and potentially increase the reaction efficiency and/or operational stability of the encapsulated proteins (Figure 10b).[31,33,85] In one example, a higher thermal tolerance was achieved for encapsulated trypsin, along with an increased reaction rate when compared to native trypsin.[31] In another example, the encapsulation of such constructs have the potential to be used to enable enzyme replacement therapies. Alternatively, these reactors can selectively uptake nanoparticles (Figure 10b) or other small molecules (Figure 10c) to enable *in situ* chemical synthesis.[85,87] For instance, nanoreactors containing poly(ethylene glycol)-*b*-poly(*α,β*-aspartic acid) (PEG-*b*-PAsp) and homo-catiomer poly([5-aminopentyl]-*α,β*-aspartamide) (Homo-PAsp-AP) were capable of activating prodrugs on location at tumor tissue sites.[85]

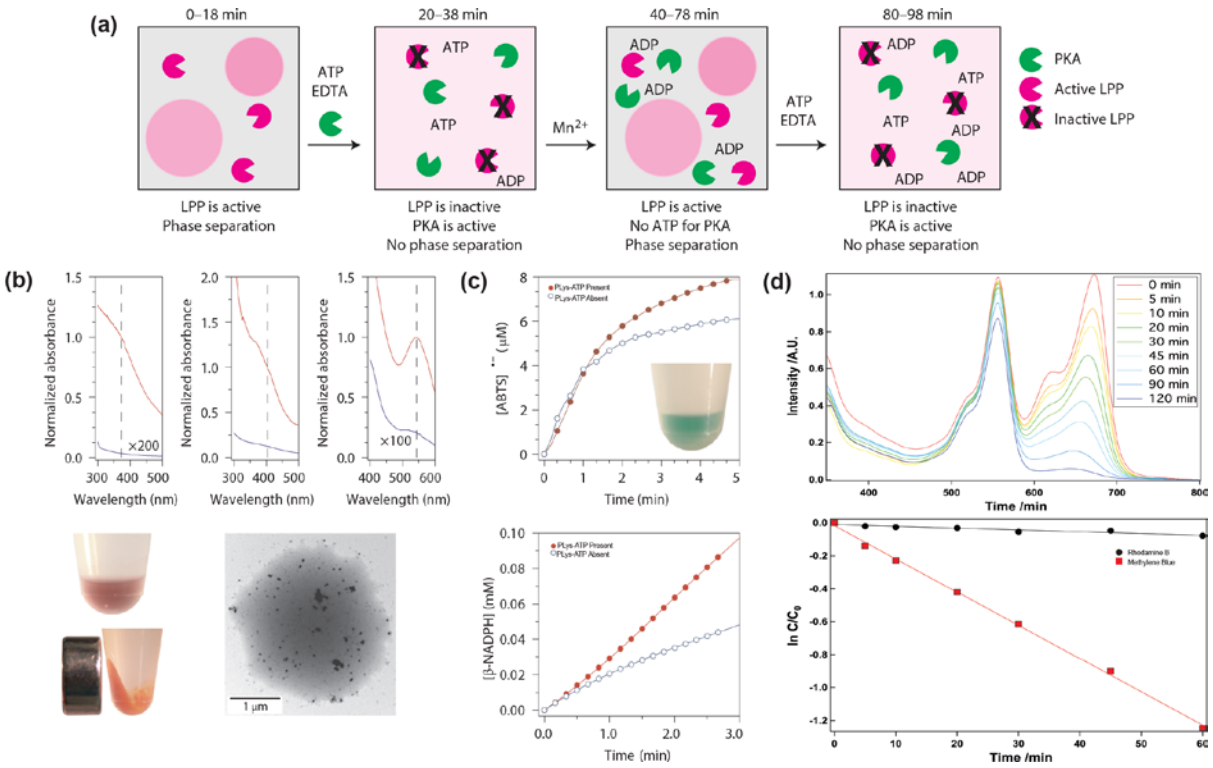

Figure 10. (a) Schematic illustration of enzyme activities during the reversible reaction using lambda protein phosphate (LPP) enzyme and protein kinase A (PKA) with adenosine diphosphate (ADP), adenosine triphosphate (ATP) and EDTA resulting in the formation and dissolution of a coacervate phase. Figure adapted with permission from Ref. [82]. (Aumiller and Keating, *Nat. Chem.*, (2015), *8*, 129-137.) **(b)** UV-vis spectra demonstrating the encapsulation of CMDex-Fe_3O_4 (left), CMDex-Co_3O_4 (middle) and gold (right) nanoparticles in poly(lysine)-adenosine triphosphate (PLys-ATP) droplets with accompanying optical images of the magnetic CMDex-Fe_3O_4 nanoparticle system and a TEM micrograph of encapsulated gold nanoparticles. **(c)** Plots of the change in concentration of (top) 2,2-azino-bis(3-ethylbenzothiazoline-6-sulfonic acid) (ABTS) and b-NADPH (bottom) as a function of time in both the presence (closed circles) and absence (open circles) of catalytic coacervate droplets. Figures adapted with permission from Ref. [30]. (Koga, *Nat. Chem.*, (2011), *3*, 720-724.) **(d)** UV-vis spectra (top) and plot of the time-dependent changes in the normalized peak intensities (bottom) for the selective catalytic degradation of methylene blue compared with rhodamine B dye as a result of selective uptake into coacervate microdroplets formed from titania nanosheets, poly(diallyldimethylammonium) chloride, and ATP. Figure adapted with permission from Ref. [87] (Lv *et al.*, *Chem. Commum.,* (2015), *51*, 8600-8602.).

Sensing:

Coacervate-based materials have been harnessed for a variety of different sensing applications. The well-defined size and aggregation number of coacervate-core micelles has facilitated their use as fluorescent nano-probes for the characterization of diffusive behavior in fluorescence recovery after photobleaching (FRAP) studies.[192,193] However, an important consideration in the development of such diffusional probes is the effect of environmental changes on the size and stability of the particle. One possibility for stabilizing such particles is through a cross-linking reaction, such as the amidation reaction that can occur at high temperatures between a carboxylate and an amine.

The controlled incorporation of lanthanide(III) ions into coacervate-core micelles has been reported for use in various imaging techniques.[115,116] Gadolinium(III) is commonly used as a contrast agent in magnetic resonance imaging (MRI), while other lanthanides such as europium(III) can be used as luminescent probes (Figure 11a-b).[115] These types of multivalent metal ions can easily be incorporated into coacervate-based materials by taking advantage of electrostatic interactions. This ease of incorporation is significant because of recent trends favoring the development of multimodal probes, such as multiple lanthanide(III) species, to combine the high resolution of MRI and the

sensitivity of optical imaging techniques. The ease of incorporating controlled quantities of multiple lanthanides into coacervate-based materials overcomes previous challenges associated with controlling the distribution of the various ions in other nanoparticle-based approaches.

Polyelectrolyte complexes have also been used directly for detection. In one example, the photoluminescence of thiophene-containing conjugated polymers in complex with double stranded DNA was used to enable quantitative DNA detection.[27] In a second example, a lamellar thin-film photonic gel was created using a poly(styrene-*b*-2-vinylpyridine) (PS-P2VP) block copolymer. The positively-charged P2VP layer allowed for the uptake of water and various proteins from solution, resulting in a change in the lamellar geometry that could be directly observed as a change in the reflected, or structural color of the film (Figure 11c-d). Differences in the size and pH-dependent charge of various proteins provided the basis for colorimetric fingerprinting and identification.[114]

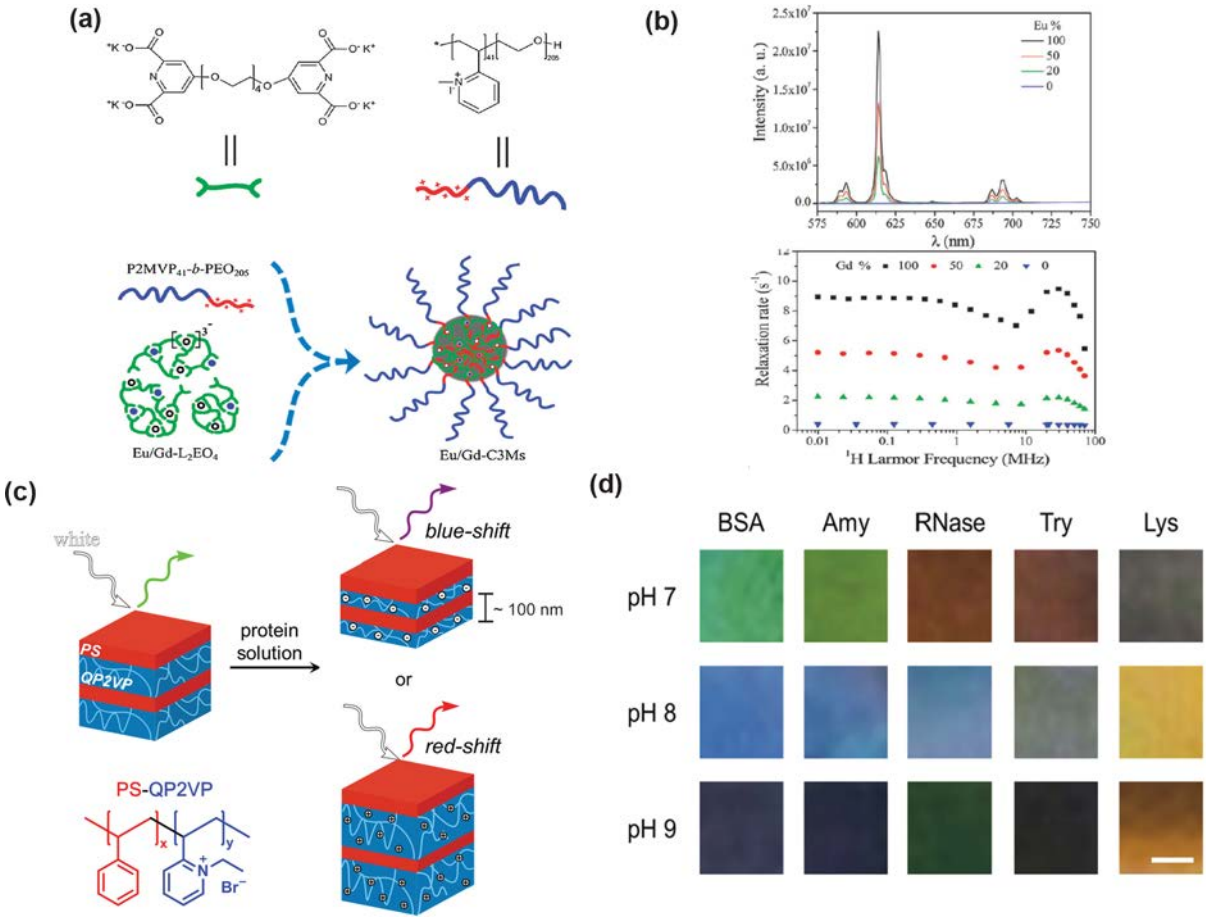

Figure 11. (a) Structure of the ligand 1,11-bis(2,6-dicarboxypyridin-4-yloxy)-3,6,9-trioxaundecane (L_2EO_4) and the diblock copolymer poly(N-methyl-2-vinyl-pyridinium iodide)-b-poly(ethylene oxide) ($P2MVP_{41}$-PEO_{205}), along with a schematic representation of the formation of the corresponding Eu/Gd-complex coacervate-core micelles (C3Ms).**(b)** Luminescent emission intensity and nuclear magnetic resonance dispersion profiles of Eu/Gd-C3Ms at different Eu^{3+}/Gd^{3+} ratios. Figure adapted with permission from Ref. [115]. (Wang *et al.*, *Chem. Commun.*, (2013), *49*, 3736.) **(c)** Schematic of the lamellar poly(styrene-*b*-2-vinylpyridine) (PS-QP2VP) photonic gel and its two possible behaviors (swelling/ contraction) in protein solutions. **(d)** Photos of PS-QP2VP photonic gels after soaking in 1% protein solutions in 10 mM Tris buffer overnight. Scale bar is 1 mm. Reprinted with permission from Fan *et al.,* (2014). Responsive Block Copolymer Photonics Triggered by Protein–Polyelectrolyte Coacervation. *ACS Nano*, *8*(11), 11467–11473. Copyright 2014. American Chemical Society. Ref. [114].

Layer-by-Layer Films:
Moving beyond the strict definition of coacervation, layer-by-layer (LbL) films are an analogous class of materials built on the concept of polyelectrolyte complexation. LbL films are assembled by the sequential deposition of oppositely-charged polyelectrolytes on a surface.[255] While complex coacervation is an equilibrium phase separation, LbL films are a kinetically-trapped assembly. Such films can be formed onto a variety of surfaces, including bubbles and droplets to create capsules for delivery. LbL assembly can be used either as a method for creating a capsule, or as a layered structure that allows for the direct release of therapeutics upon disassembly. Careful design of the layered structures can enable both spatial and temporal control over the release of therapeutics. Alternatively, the materials of the films themselves could be harnessed as active coatings, such as antibacterial and/or antifouling surfaces.[113] However, an in-depth discussion of LbL films is beyond the scope of this article. We refer the readers to several other recent review articles on the topic.[256-259]

Solid Polyelectrolyte Complexes:
While LbL films can be formed as free-standing films, they are much more commonly presented as coatings. However, recent reports have demonstrated the utility of bulk polyelectrolyte complex solids as well. Unlike coacervates, polyelectrolyte complexes were historically considered intractable, as they were resistant to either solvent or thermal processing.[6,260] Instead, the presence of both salt and water has been shown to enable plasticization of these “saloplastic” materials. The biocompatibility of these materials should follow based on the properties of the individual components, as with complex coacervates. Compacted saloplastic materials typically show extensive porosity and mechanical properties that make them attractive as materials for bioimplants such as cartilage mimics,[261] or replacement materials for the nucleus pulposus in intervertebral disks,[262] as well as tissue culture scaffolds, supports for biocatalysis, and drug delivery vehicles.[260] However, thus far saloplastic materials have only been reported for synthetic polymer systems. Expanding this class of materials to include biopolyelectrolytes such as proteins, hyaluronic acid, chitosan, or chondroitin sulfate has tremendous potential to further enhance their utility. A more detailed discussion of these materials is beyond the scope of this article, and we refer readers to a recent review article on the subject.[260]

Conclusion

Complex coacervates have been gaining interest in various fields owing to their tunability, biocompatibility, and wide range of utility in medical applications and beyond. The strength of complex coacervates lies in their ability to encapsulate and stabilize a wide range of cargoes, including hydrophilic molecules. Furthermore, this encapsulation can be performed in a fully aqueous environment while taking advantage of a vast diversity of both natural and synthetic polyelectrolyte materials. This combination of factors favors coacervate-based materials in the development of delivery platforms, sensors, and other compartmentalized structures ranging from drug delivery to green catalysis. In fact, coacervate-based materials have progressed into Stage I clinical trials for the delivery of cisplatin to solid tumors.[212]

However, widespread success of coacervate-based materials across diverse applications requires a strong foundational understanding of complex coacervate self-assembly. This is a particular challenge as the field looks to harness increasingly complex molecular systems. In addition to ionic

strength and pH control, new efforts are focusing on understanding the effects of molecular topology, chemical sequence, orthogonal interactions such as hydrogen bonding, and more complex three-dimensional structures. Additional experimental and computational efforts are critical to continue the development of this field, and an emphasis must be placed on establishing a broad, molecular-level understanding of coacervation in general. While many experimental reports have taken advantage of naturally occurring biopolymers, it is critical to use well-defined model systems to understand the basic physical phenomena, and then determine how to translate these results to more realistic, less chemically or physically well-defined material systems. This level of predictive understanding would enable the intelligent design of a diverse array of materials and help to open up new and exciting avenues for exploration and development.

References

(1) Perry, S.; Li, Y.; Priftis, D.; Leon, L.; Tirrell, M. The effect of salt on the complex coacervation of vinyl polyelectrolytes. *Polymers* **2014**, *6* (6), 1756–1772 DOI: 10.3390/polym6061756.

(2) Priftis, D.; Leon, L.; Song, Z.; Perry, S. L.; Margossian, K. O.; Tropnikova, A.; Cheng, J.; Tirrell, M. Self-assembly of α-helical polypeptides driven by complex coacervation. *Angew. Chem.* **2015**, *127* (38), 11280–11284 DOI: 10.1002/ange.201504861.

(3) Water, J. J.; Schack, M. M.; Velazquez-Campoy, A.; Maltesen, M. J.; van de Weert, M.; Jorgensen, L. Complex coacervates of hyaluronic acid and lysozyme: effect on protein structure and physical stability. *Eur. J. Pharm. Biopharm.* **2014**, *88* (2), 325–331 DOI: 10.1016/j.ejpb.2014.09.001.

(4) Black, K. A.; Priftis, D.; Perry, S. L.; Yip, J.; Byun, W. Y.; Tirrell, M. Protein encapsulation via polypeptide complex coacervation. *ACS Macro Lett.* **2014**, *3* (10), 1088–1091 DOI: 10.1021/mz500529v.

(5) Kim, S.; Huang, J.; Lee, Y.; Dutta, S.; Yoo, H. Y.; Jung, Y. M.; Jho, Y.; Zeng, H.; Hwang, D. S. Complexation and coacervation of like-charged polyelectrolytes inspired by mussels. *PNAS* **2016**, *113* (7), E847–E853 DOI: 10.1073/pnas.1521521113.

(6) Wang, Q.; Schlenoff, J. B. The polyelectrolyte complex/coacervate continuum. *Macromolecules* **2014**, *47* (9), 3108–3116 DOI: 10.1021/ma500500q.

(7) Frankel, E. A.; Bevilacqua, P. C.; Keating, C. D. Polyamine/Nucleotide coacervates provide strong compartmentalization of Mg 2+, nucleotides, and RNA. *Langmuir* **2016**, *32* (8), 2041–2049 DOI: 10.1021/acs.langmuir.5b04462.

(8) Tang, T. Y. D.; Antognozzi, M.; Vicary, J. A.; Perriman, A. W.; Mann, S. Small-molecule uptake in membrane-free peptide/nucleotide protocells. *Soft Matter* **2013**, *9* (31), 7647–7656 DOI: 10.1039/c3sm50726b.

(9) Hwang, D. S.; Waite, J. H.; Tirrell, M. Promotion of osteoblast proliferation on complex coacervation-based hyaluronic acid–recombinant mussel adhesive protein coatings on titanium. *Biomaterials* **2010**, *31* (6), 1080–1084 DOI: 10.1016/j.biomaterials.2009.10.041.

(10) Kizilay, E.; Kayitmazer, A. B.; Dubin, P. L. Complexation and coacervation of polyelectrolytes with oppositely charged colloids. *Adv. Colloid Interface Sci.* **2011**, *167* (1-2), 24–37 DOI: 10.1016/j.cis.2011.06.006.

(11) Dubin, P. L.; Li, Y.; Jaeger, W. Mesophase separation in polyelectrolyte-mixed micelle coacervates. *Langmuir* **2008**, *24* (9), 4544–4549 DOI: 10.1021/la702405d.

(12) Ifeduba, E. A.; Akoh, C. C. Microencapsulation of stearidonic acid soybean oil in Maillard reaction-modified complex coacervates. *Food Chem.* **2016**, *199* (C), 524–532 DOI: 10.1016/j.foodchem.2015.12.011.

(13) Hoffmann, K. Q.; Perry, S. L.; Leon, L.; Priftis, D.; Tirrell, M.; de Pablo, J. J. A molecular view of the role of chirality in charge-driven polypeptide complexation. *Soft Matter* **2015**, *11*, 1525–1538 DOI: 10.1039/C4SM02336F.

(14) Perry, S. L.; Leon, L.; Hoffmann, K. Q.; Kade, M. J.; Priftis, D.; Black, K. A.; Wong, D.; Klein, R. A.; Pierce, C. F.; Margossian, K. O.; et al. Chirality-selected phase behaviour in ionic polypeptide complexes. *Nat. Commun.* **2015**, *6*, 6052 DOI: 10.1038/ncomms7052.

(15) Obermeyer, A. C.; Mills, C. E.; Dong, X.-H.; Flores, R. J.; Olsen, B. D. Complex coacervation of supercharged proteins with polyelectrolytes. *Soft Matter* **2016**, *12*, 3570–3581 DOI:

10.1039/C6SM00002A.
(16) Pippa, N.; Karayianni, M.; Pispas, S.; Demetzos, C. Complexation of cationic-neutral block polyelectrolyte with insulin and in vitro release studies. *Int. J. Pharm.* **2015**, *491* (1-2), 136–143 DOI: 10.1016/j.ijpharm.2015.06.013.
(17) Pippa, N.; Kalinova, R.; Dimitrov, I.; Pispas, S.; Demetzos, C. Insulin/poly(ethylene glycol)- block-poly(l-lysine) Complexes: Physicochemical Properties and Protein Encapsulation. *J. Phys. Chem. B* **2015**, *119* (22), 6813–6819 DOI: 10.1021/acs.jpcb.5b01664.
(18) Nolles, A.; Westphal, A. H.; de Hoop, J. A.; Fokkink, R. G.; Kleijn, J. M.; van Berkel, W. J. H.; Borst, J. W.; Westphal, A. H. Encapsulation of GFP in complex coacervate core micelles. *Biomacromolecules* **2015**, *16* (5), 1542–1549 DOI: 10.1021/acs.biomac.5b00092.
(19) Chen, W. C. W.; Lee, B. G.; Park, D. W.; Kim, K.; Chu, H.; Kim, K.; Huard, J.; Wang, Y. Controlled dual delivery of fibroblast growth factor-2 and Interleukin-10 by heparin-based coacervate synergistically enhances ischemic heart repair. *Biomaterials* **2015**, *72* (c), 138–151 DOI: 10.1016/j.biomaterials.2015.08.050.
(20) Bungenberg de Jong, H.; Kruyt, H. R. Koazervation. *Kolloid-Z.* **1930**, *50* (1), 39–48.
(21) Turgeon, S. L.; Schmitt, C.; Sanchez, C. Protein–polysaccharide complexes and coacervates. *Curr. Opin. Colloid Interface Sci.* **2007** DOI: 10.1016/j.cocis.2007.07.007.
(22) Schmitt, C.; Turgeon, S. L. Protein/polysaccharide complexes and coacervates in food systems. *Adv. Colloid Interface Sci.* **2011**, *167* (1-2), 63–70 DOI: 10.1016/j.cis.2010.10.001.
(23) Yeo, Y.; Bellas, E.; Firestone, W.; Langer, R.; Kohane, D. S. Complex coacervates for thermally sensitive controlled release of flavor compounds. *J. Agric. Food Chem.* **2005**, *53* (19), 7518–7525 DOI: 10.1021/jf0507947.
(24) Matalanis, A.; Jones, O. G.; McClements, D. J. Structured biopolymer-based delivery systems for encapsulation, protection, and release of lipophilic compounds. *Food Hydrocolloids* **2011**, *25* (8), 1865–1880 DOI: 10.1016/j.foodhyd.2011.04.014.
(25) Jourdain, L.; Leser, M. E.; Schmitt, C.; Michel, M.; Dickinson, E. Stability of emulsions containing sodium caseinate and dextran sulfate: relationship to complexation in solution. *Food Hydrocolloids* **2008**, *22* (4), 647–659 DOI: 10.1016/j.foodhyd.2007.01.007.
(26) Weinbreck, F.; de Vries, R.; Schrooyen, P.; de Kruif, C. G. Complex coacervation of whey proteins and gum arabic. *Biomacromolecules* **2003**, *4* (2), 293–303 DOI: 10.1021/bm025667n.
(27) Knaapila, M.; Costa, T.; Garamus, V. M.; Kraft, M.; Drechsler, M.; Scherf, U.; Burrows, H. D. Polyelectrolyte complexes of a cationic all conjugated fluorene–thiophene diblock copolymer with aqueous DNA. *J. Phys. Chem. B* **2015**, *119* (7), 3231–3241 DOI: 10.1021/jp5110032.
(28) Arfin, N.; Aswal, V. K.; Bohidar, H. B. Overcharging, thermal, viscoelastic and hydration properties of DNA–gelatin complex coacervates: pharmaceutical and food industries. *RSC Adv.* **2014**, *4* (23), 11705–11709 DOI: 10.1039/c3ra46618c.
(29) Williams, D. S.; Koga, S.; Hak, C. R. C.; Majrekar, A.; Patil, A. J.; Perriman, A. W.; Mann, S. Polymer/nucleotide droplets as bio-inspired functional micro-compartments. *Soft Matter* **2012**, *8* (22), 6004–6011 DOI: 10.1039/c2sm25184a.
(30) Koga, S.; Williams, D. S.; Perriman, A. W.; Mann, S. Peptide-nucleotide microdroplets as a step towards a membrane-free protocell model. *Nat. Chem.* **2011**, *3* (9), 720–724 DOI: 10.1038/nchem.1110.
(31) Kawamura, A.; Harada, A.; Kono, K.; Kataoka, K. Self-assembled nano-bioreactor from block ionomers with elevated and stabilized enzymatic function. *Bioconjugate Chem.* **2007**, *18* (5), 1555–1559 DOI: 10.1021/bc070029t.
(32) Jaturanpinyo, M.; Harada, A.; Yuan, X.; Kataoka, K. Preparation of bionanoreactor based on core−shell structured polyion complex micelles entrapping trypsin in the core cross-linked with glutaraldehyde. *Bioconjugate Chem.* **2004**, *15* (2), 344–348 DOI: 10.1021/bc034149m.
(33) Kataoka, K.; Harada, A. Pronounced activity of enzymes through the incorporation into the core of polyion complex micelles made from charged block copolymers. *J. Controlled Release* **2001**, *72*, 85–91.
(34) Kataoka, K.; Harada, A.; Nagasaki, Y. Block copolymer micelles for drug delivery: design, characterization and biological significance. *Adv. Drug Delivery Rev.* **2001**, *47*, 113–131.
(35) Harada, A.; Kataoka, K. Novel polyion complex micelles entrapping enzyme molecules in the core. 2. characterization of the micelles prepared at nonstoichiometric mixing ratios. *Langmuir* **1999**, *15* (12), 4208–4212 DOI: 10.1021/la981087t.
(36) Harada, A.; Kataoka, K. Novel polyion complex micelles entrapping enzyme molecules in the core:

preparation of narrowly-distributed micelles from lysozyme and poly(ethylene glycol)-poly(aspartic acid) block copolymer in aqueous medium. *Macromolecules* **1998**, *31*, 288–294.

(37) Harada, A.; Kataoka, K. Formation of polyion complex micelles in an aqueous milieu from a pair of oppositely-charged block copolymers with poly(ethylene glycol) segments. *Macromolecules* **1995**, *28*, 5294–5299.

(38) Voets, I. K.; de Keizer, A.; Cohen Stuart, M. A. Complex coacervate core micelles. *Adv. Colloid Interface Sci.* **2009**, *147-148* (C), 300–318 DOI: 10.1016/j.cis.2008.09.012.

(39) Kayitmazer, A. B.; Seyrek, E.; Dubin, P. L.; Staggemeier, B. A. Influence of chain stiffness on the interaction of polyelectrolytes with oppositely charged micelles and proteins. *J. Phys. Chem. B* **2003**, *107* (32), 8158–8165 DOI: 10.1021/jp034065a.

(40) Kalantar, T. H.; Tucker, C. J.; Zalusky, A. S.; Boomgaard, T. A.; Wilson, B. E.; Ladika, M.; Jordan, S. L.; Li, W. K.; Zhang, X.; Goh, C. G. High throughput workflow for coacervate formation and characterization in shampoo systems. *J. Cosmet. Sci.* **2007**, *58*, 375–383.

(41) Hu, D.; Chou, K. C. Re-evaluating the surface tension analysis of polyelectrolyte-surfactant mixtures using phase-sensitive sum frequency generation spectroscopy. *JACS* **2014**, *136* (43), 15114–15117 DOI: 10.1021/ja5049175.

(42) Nejati, M. M.; Khaledi, M. G. Perfluoro-alcohol-induced complex coacervates of polyelectrolyte–surfactant mixtures: Phase behavior and analysis. *Langmuir* **2015**, *31* (20), 5580–5589 DOI: 10.1021/acs.langmuir.5b00444.

(43) Szczepanowicz, K.; Bazylińska, U.; Pietkiewicz, J.; Szyk-Warszyńska, L.; Wilk, K. A.; Warszyński, P. Biocompatible long-sustained release oil-core polyelectrolyte nanocarriers: From controlling physical state and stability to biological impact. *Adv. Colloid Interface Sci.* **2015**, *222* (C), 678–691 DOI: 10.1016/j.cis.2014.10.005.

(44) Wang, Y.; Kimura, K.; Huang, Q.; Dubin, P. L.; Jaeger, W. Effects of salt on polyelectrolyte−micelle coacervation. *Macromolecules* **1999**, *32* (21), 7128–7134 DOI: 10.1021/ma990972v.

(45) Wang, W.; Mauroy, H.; Zhu, K.; Knudsen, K. D.; Kjøniksen, A.-L.; Nyström, B.; Sande, S. A. Complex coacervate micelles formed by a C18-capped cationic triblock thermoresponsive copolymer interacting with SDS. *Soft Matter* **2012**, *8* (45), 11514–11525 DOI: 10.1039/c2sm26567b.

(46) Karimi, F.; Qazvini, N. T.; Namivandi-Zangeneh, R. Fish gelatin/laponite biohybrid elastic coacervates: a complexation kinetics–structure relationship study. *Int. J. Biol. Macromol.* **2013**, *61*, 102–113 DOI: 10.1016/j.ijbiomac.2013.06.054.

(47) Pawar, N.; Bohidar, H. B. Anisotropic domain growth and complex coacervation in nanoclay-polyelectrolyte solutions. *Adv. Colloid Interface Sci.* **2011**, *167* (1-2), 12–23 DOI: 10.1016/j.cis.2011.06.007.

(48) Krogstad, D. V.; Lynd, N. A.; Choi, S.-H.; Spruell, J. M.; Hawker, C. J.; Kramer, E. J.; Tirrell, M. V. Effects of polymer and salt concentration on the structure and properties of triblock copolymer coacervate hydrogels. *Macromolecules* **2013**, *46* (4), 1512–1518 DOI: 10.1021/ma302299r.

(49) Krogstad, D. V.; Choi, S.-H.; Lynd, N. A.; Audus, D. J.; Perry, S. L.; Gopez, J. D.; Hawker, C. J.; Kramer, E. J.; Tirrell, M. V. Small angle neutron scattering study of complex coacervate micelles and hydrogels formed from ionic diblock and triblock copolymers. *J. Phys. Chem. B* **2014**, *118* (45), 13011–13018 DOI: 10.1021/jp509175a.

(50) Krogstad, D. V.; Lynd, N. A.; Miyajima, D.; Gopez, J.; Hawker, C. J.; Kramer, E. J.; Tirrell, M. V. Structural evolution of polyelectrolyte complex core micelles and ordered-phase bulk materials. *Macromolecules* **2014**, *47* (22), 8026–8032 DOI: 10.1021/ma5017852.

(51) Hunt, J. N.; Feldman, K. E.; Lynd, N. A.; Deek, J.; Campos, L. M.; Spruell, J. M.; Hernandez, B. M.; Kramer, E. J.; Hawker, C. J. Tunable, high modulus hydrogels driven by ionic coacervation. *Adv. Mater.* **2011**, *23* (20), 2327–2331 DOI: 10.1002/adma.201004230.

(52) Stewart-Sloan, C. R.; Olsen, B. D. Protonation-induced microphase separation in thin films of a polyelectrolyte-hydrophilic diblock copolymer. *ACS Macro Lett.* **2014**, *3* (5), 410–414 DOI: 10.1021/mz400650q.

(53) Kim, B.; Lam, C. N.; Olsen, B. D. Nanopatterned protein films directed by ionic complexation with water-soluble diblock copolymers. *Macromolecules* **2012**, *45* (11), 4572–4580 DOI: 10.1021/ma2024914.

(54) Wu, F.-G.; Jiang, Y.-W.; Chen, Z.; Yu, Z.-W. Folding behaviors of protein (lysozyme) confined in polyelectrolyte complex micelle. *Langmuir* **2016**, *32* (15), 3655–3664 DOI: 10.1021/acs.langmuir.6b00235.

(55) Ishii, S.; Kaneko, J.; Nagasaki, Y. Development of a long-acting, protein-loaded, redox-active,

injectable gel formed by a polyion complex for local protein therapeutics. *Biomaterials* **2016**, *84* (C), 210–218 DOI: 10.1016/j.biomaterials.2016.01.029.

(56) Wang, W.; Xu, Y.; Li, A.; Li, T.; Liu, M.; Klitzing, von, R.; Ober, C. K.; Kayitmazer, A. B.; Li, L.; Guo, X. Zinc induced polyelectrolyte coacervate bioadhesive and its transition to a self-healing hydrogel. *RSC Adv.* **2015**, *5*, 66871–66878 DOI: 10.1039/C5RA11915D.

(57) Winslow, B. D.; Shao, H.; Stewart, R. J.; Tresco, P. A. Biocompatibility of adhesive complex coacervates modeled after the sandcastle glue of Phragmatopoma californica for craniofacial reconstruction. *Biomaterials* **2010**, *31* (36), 9373–9381 DOI: 10.1016/j.biomaterials.2010.07.078.

(58) Favi, P. M.; Yi, S.; Lenaghan, S. C.; Xia, L.; Zhang, M. Inspiration from the natural world: from bio-adhesives to bio-inspired adhesives. *J. Adhes. Sci. Technol.* **2013**, *28* (3-4), 290–319 DOI: 10.1080/01694243.2012.691809.

(59) Mann, L. K.; Papanna, R.; Moise, K. J., Jr; Byrd, R. H.; Popek, E. J.; Kaur, S.; Tseng, S. C. G.; Stewart, R. J. Fetal membrane patch and biomimetic adhesive coacervates as a sealant for fetoscopic defects. *Acta Biomater.* **2012**, *8* (6), 2160–2165 DOI: 10.1016/j.actbio.2012.02.014.

(60) Lim, S.; Choi, Y. S.; Kang, D. G.; Song, Y. H.; Cha, H. J. The adhesive properties of coacervated recombinant hybrid mussel adhesive proteins. *Biomaterials* **2010**, *31* (13), 3715–3722 DOI: 10.1016/j.biomaterials.2010.01.063.

(61) Hwang, D. S.; Zeng, H.; Srivastava, A.; Krogstad, D. V.; Tirrell, M.; Israelachvili, J. N.; Waite, J. H. Viscosity and interfacial properties in a mussel-inspired adhesive coacervate. *Soft Matter* **2010**, *6* (14), 3232–3235 DOI: 10.1039/c002632h.

(62) Hwang, D. S.; Zeng, H.; Lu, Q.; Israelachvili, J.; Waite, J. H. Adhesion mechanism in a DOPA-deficient foot protein from green mussels. *Soft Matter* **2012**, *8* (20), 5640–5649 DOI: 10.1039/c2sm25173f.

(63) Kaur, S.; Weerasekare, G. M.; Stewart, R. J. Multiphase adhesive coacervates inspired by the sandcastle worm. *ACS Appl. Mater. Interfaces* **2011**, *3* (4), 941–944 DOI: 10.1021/am200082v.

(64) Ahn, B. K.; Das, S.; Linstadt, R.; Kaufman, Y.; Martinez-Rodriguez, N. R.; Mirshafian, R.; Kesselman, E.; Talmon, Y.; Lipshutz, B. H.; Israelachvili, J. N.; et al. High-performance mussel-inspired adhesives of reduced complexity. *Nat. Commun.* **2015**, *6*, 8663 DOI: 10.1038/ncomms9663.

(65) Stewart, R. J.; Wang, C. S.; Shao, H. Complex coacervates as a foundation for synthetic underwater adhesives. *Adv. Colloid Interface Sci.* **2011**, *167* (1-2), 85–93 DOI: 10.1016/j.cis.2010.10.009.

(66) Choi, Y. S.; Kang, D. G.; Lim, S.; Yang, Y. J.; Kim, C. S.; Cha, H. J. Recombinant mussel adhesive protein fp-5 (MAP fp-5) as a bulk bioadhesive and surface coating material. *Biofouling* **2011**, *27* (7), 729–737 DOI: 10.1080/08927014.2011.600830.

(67) Shao, H.; Bachus, K. N.; Stewart, R. J. A water-borne adhesive modeled after the sandcastle glue of P. californica. *Macromol. Biosci.* **2009**, *9* (5), 464–471 DOI: 10.1002/mabi.200800252.

(68) Lim, S.; Moon, D.; Kim, H. J.; Seo, J. H.; Kang, I. S.; Cha, H. J. Interfacial tension of complex coacervated mussel adhesive protein according to the Hofmeister series. *Langmuir* **2014**, *30* (4), 1108–1115 DOI: 10.1021/la403680z.

(69) Shao, H.; Weerasekare, G. M.; Stewart, R. J. Controlled curing of adhesive complex coacervates with reversible periodate carbohydrate complexes. *J. Biomed. Mater. Res., Part A* **2011**, *97A* (1), 46–51 DOI: 10.1002/jbm.a.33026.

(70) Farrar, D. F. Bone adhesives for trauma surgery a review of challenges and developments. *Int. J. Adhes. Adhes.* **2012**, *33* (C), 89–97 DOI: 10.1016/j.ijadhadh.2011.11.009.

(71) Lindhoud, S.; de Vries, R.; Norde, W.; Cohen Stuart, M. A. Structure and stability of complex coacervate core micelles with lysozyme. *Biomacromolecules* **2007**, *8* (7), 2219–2227 DOI: 10.1021/bm0700688.

(72) Lindhoud, S.; Claessens, M. M. A. E. Accumulation of small protein molecules in a macroscopic complex coacervate. *Soft Matter* **2015**, *12* (2), 408–413 DOI: 10.1039/C5SM02386F.

(73) Kishimura, A.; Koide, A.; Osada, K.; Yamasaki, Y.; Kataoka, K. Encapsulation of myoglobin in PEGylated polyion complex vesicles made from a pair of oppositely charged block ionomers: a physiologically available oxygen carrier. *Angew. Chem. Int. Ed.* **2007**, *46* (32), 6085–6088 DOI: 10.1002/anie.200701776.

(74) Lindhoud, S.; de Vries, R.; Schweins, R.; Cohen Stuart, M. A.; Norde, W. Salt-induced release of lipase from polyelectrolyte complex micelles. *Soft Matter* **2009**, *5* (1), 242–250 DOI: 10.1039/B811640G.

(75) Lindhoud, S.; Norde, W.; Cohen Stuart, M. A. Reversibility and relaxation behavior of polyelectrolyte complex micelle formation. *J. Phys. Chem. B* **2009**, *113* (16), 5431–5439 DOI: 10.1021/jp809489f.

(76) Chu, H.; Gao, J.; Chen, C.-W.; Huard, J.; Wang, Y. Injectable fibroblast growth factor-2 coacervate for persistent angiogenesis. *PNAS* **2011**, *108* (33), 13444–13449 DOI: 10.1073/pnas.1110121108.
(77) Johnson, N. R.; Ambe, T.; Wang, Y. Lysine-based polycation:heparin coacervate for controlled protein delivery. *Acta Biomater.* **2014**, *10* (1), 40–46 DOI: 10.1016/j.actbio.2013.09.012.
(78) Chu, H.; Chen, C.-W.; Huard, J.; Wang, Y. The effect of a heparin-based coacervate of fibroblast growth factor-2 on scarring in the infarcted myocardium. *Biomaterials* **2013**, *34* (6), 1747–1756 DOI: 10.1016/j.biomaterials.2012.11.019.
(79) Yen, J.; Ying, H.; Wang, H.; Yin, L.; Uckun, F.; Cheng, J. CD44 mediated nonviral gene delivery into human embryonic stem cells via hyaluronic-acid-coated nanoparticles. *ACS Biomater. Sci. Eng.* **2016**, *2* (3), 326–335 DOI: 10.1021/acsbiomaterials.5b00393.
(80) Perry, S. L.; Neumann, S. G.; Neumann, T.; Cheng, K.; Ni, J.; Weinstein, J. R.; Schaffer, D. V.; Tirrell, M. Challenges in nucleic acid-lipid films for transfection. *AIChE J.* **2013**, *59* (9), 3203–3213 DOI: 10.1002/aic.14198.
(81) Kuo, C.-H.; Leon, L.; Chung, E. J.; Huang, R.-T.; Sontag, T. J.; Reardon, C. A.; Getz, G. S.; Tirrell, M.; Fang, Y. Inhibition of atherosclerosis-promoting microRNAs via targeted polyelectrolyte complex micelles. *J. Mater. Chem. B* **2014**, *2*, 8142–8153 DOI: 10.1039/C4TB00977K.
(82) Aumiller, W. M., Jr; Keating, C. D. Phosphorylation-mediated RNA/peptide complex coacervation as a model for intracellular liquid organelles. *Nat. Chem.* **2015**, *8* (2), 129–137 DOI: 10.1038/nchem.2414.
(83) Jin, K.-M.; Kim, Y.-H. Injectable, thermo-reversible and complex coacervate combination gels for protein drug delivery. *J. Controlled Release* **2008**, *127* (3), 249–256 DOI: 10.1016/j.jconrel.2008.01.015.
(84) Kinoh, H.; Miura, Y.; Chida, T.; Liu, X.; Mizuno, K.; Fukushima, S.; Morodomi, Y.; Nishiyama, N.; Cabral, H.; Kataoka, K. Nanomedicines eradicating cancer stem-like cells in vivo by pH-triggered intracellular cooperative action of loaded drugs. *ACS Nano* **2016**, *10* (6), 5643–5655 DOI: 10.1021/acsnano.6b00900.
(85) Anraku, Y.; Kishimura, A.; Kamiya, M.; Tanaka, S.; Nomoto, T.; Toh, K.; Matsumoto, Y.; Fukushima, S.; Sueyoshi, D.; Kano, M. R.; et al. Systemically injectable enzyme-loaded polyion complex vesicles as in vivo nanoreactors functioning in tumors. *Angew. Chem.* **2015**, *128* (2), 570–575 DOI: 10.1002/ange.201508339.
(86) Schoonen, L.; van Hest, J. C. M. Compartmentalization approaches in soft matter science: From nanoreactor development to organelle mimics. *Adv. Mater.* **2015**, *28* (6), 1109–1128 DOI: 10.1002/adma.201502389.
(87) Lv, K.; Perriman, A. W.; Mann, S. Photocatalytic multiphase micro-droplet reactors based on complex coacervation. *Chem. Commun.* **2015**, *51*, 8600–8602 DOI: 10.1039/C5CC01914A.
(88) Hyman, A. A.; Simons, K. Beyond oil and water--phase transitions in cells. *Science* **2012**, *337* (6098), 1047–1049 DOI: 10.1126/science.1223728.
(89) Hyman, A. A.; Brangwynne, C. P. Beyond stereospecificity: liquids and mesoscale organization of cytoplasm. *Dev. Cell* **2011**, *21* (1), 14–16 DOI: 10.1016/j.devcel.2011.06.013.
(90) Weber, S. C.; Brangwynne, C. P. Getting RNA and protein in phase. *Cell* **2012**, *149* (6), 1188–1191 DOI: 10.1016/j.cell.2012.05.022.
(91) Elbaum-Garfinkle, S.; Kim, Y.; Szczepaniak, K.; Chen, C. C.-H.; Eckmann, C. R.; Myong, S.; Brangwynne, C. P. The disordered P granule protein LAF-1 drives phase separation into droplets with tunable viscosity and dynamics. *PNAS* **2015**, *112* (23), 7189–7194 DOI: 10.1073/pnas.1504822112.
(92) Kato, M.; Han, T. W.; Xie, S.; Shi, K.; Du, X.; Wu, L. C.; Mirzaei, H.; Goldsmith, E. J.; Longgood, J.; Pei, J.; et al. Cell-free formation of RNA granules: low complexity sequence domains form dynamic fibers within hydrogels. *Cell* **2012**, *149* (4), 753–767 DOI: 10.1016/j.cell.2012.04.017.
(93) Eulalio, A.; Behm-Ansmant, I.; Izaurralde, E. P bodies: at the crossroads of post-transcriptional pathways. *Nat. Rev. Mol. Cell Biol.* **2007**, *8* (1), 9–22 DOI: 10.1038/nrm2080.
(94) Han, T. W.; Kato, M.; Xie, S.; Wu, L. C.; Mirzaei, H.; Pei, J.; Chen, M.; Xie, Y.; Allen, J.; Xiao, G.; et al. Cell-free formation of RNA granules: bound RNAs identify features and components of cellular assemblies. *Cell* **2012**, *149* (4), 768–779 DOI: 10.1016/j.cell.2012.04.016.
(95) Jia, T. Z.; Hentrich, C.; Szostak, J. W. Rapid RNA exchange in aqueous two-phase system and coacervate droplets. *Origins Life Evol. Biospheres* **2014**, *44* (1), 1–12 DOI: 10.1007/s11084-014-9355-8.
(96) Li, P.; Banjade, S.; Cheng, H.-C.; Kim, S.; Chen, B.; Guo, L.; Llaguno, M.; Hollingsworth, J. V.; King, D.

S.; Banani, S. F.; et al. Phase transitions in the assembly of multivalent signalling proteins. *Nature* **2012**, *483* (7389), 336–340 DOI: 10.1038/nature10879.
(97) Walter, H. Consequences of Phase Separation in Cytoplasm. *Int. Rev. Cytol.* **1999**, *192*, 331–343.
(98) Brangwynne, C. P.; Mitchison, T. J.; Hyman, A. A. Active liquid-like behavior of nucleoli determines their size and shape in Xenopus laevis oocytes. *PNAS* **2011**, *108* (11), 4334–4339 DOI: 10.1073/pnas.1017150108.
(99) Brangwynne, C. P.; Eckmann, C. R.; Courson, D. S.; Rybarska, A.; Hoege, C.; Gharakhani, J.; Julicher, F.; Hyman, A. A. Germline P Granules are liquid droplets that localize by controlled dissolution/condensation. *Science* **2009**, *324* (5935), 1729–1732 DOI: 10.1126/science.1172046.
(100) Brangwynne, C. P. Phase transitions and size scaling of membrane-less organelles. *J. Cell. Biol.* **2013**, *203* (6), 875–881 DOI: 10.1083/jcb.201308087.
(101) Zhang, H.; Elbaum-Garfinkle, S.; Langdon, E. M.; Taylor, N.; Occhipinti, P.; Bridges, A. A.; Brangwynne, C. P.; Gladfelter, A. S. RNA controls PolyQ protein phase transitions. *Mol. Cell* **2015**, *60* (2), 220–230 DOI: 10.1016/j.molcel.2015.09.017.
(102) Lin, Y.; Protter, D. S. W.; Rosen, M. K.; Parker, R. Formation and maturation of phase-separated liquid droplets by RNA-binding proteins. *Mol. Cell* **2015**, *60* (2), 208–219 DOI: 10.1016/j.molcel.2015.08.018.
(103) Fromm, S. A.; Kamenz, J.; Nöldeke, E. R.; Neu, A.; Zocher, G.; Sprangers, R. In vitro reconstitution of a cellular phase-transition process that Involves the mRNA decapping machinery. *Angew. Chem. Int. Ed.* **2014**, *53* (28), 7354–7359 DOI: 10.1002/anie.201402885.
(104) Patel, A.; Lee, H. O.; Jawerth, L.; Maharana, S.; Jahnel, M.; Hein, M. Y.; Stoynov, S.; Mahamid, J.; Saha, S.; Franzmann, T. M.; et al. A liquid-to-solid phase transition of the ALS protein FUS accelerated by disease mutation. *Cell* **2015**, *162* (5), 1066–1077 DOI: 10.1016/j.cell.2015.07.047.
(105) Burke, K. A.; Janke, A. M.; Rhine, C. L.; Fawzi, N. L. Residue-by-residue view of in vitro FUS granules that bind the C-terminal domain of RNA polymerase II. *Mol. Cell* **2015**, *60* (2), 231–241 DOI: 10.1016/j.molcel.2015.09.006.
(106) Vehlow, D.; Schmidt, R.; Gebert, A.; Siebert, M.; Lips, K.; Müller, M. Polyelectrolyte complex based interfacial drug delivery system with controlled loading and improved release performance for bone therapeutics. *Nanomaterials* **2016**, *6* (3), 53–21 DOI: 10.3390/nano6030053.
(107) Rauck, B. M.; Novosat, T. L.; Oudega, M.; Wang, Y. Biocompatibility of a coacervate-based controlled release system for protein delivery to the injured spinal cord. *Acta Biomater.* **2015**, *11* (C), 204–211 DOI: 10.1016/j.actbio.2014.09.037.
(108) Lee, K.-W.; Johnson, N. R.; Gao, J.; Wang, Y. Human progenitor cell recruitment via SDF-1α coacervate-laden PGS vascular grafts. *Biomaterials* **2013**, *34* (38), 9877–9885 DOI: 10.1016/j.biomaterials.2013.08.082.
(109) Priftis, D.; Farina, R.; Tirrell, M. Interfacial energy of polypeptide complex coacervates measured via capillary adhesion. *Langmuir* **2012**, *28* (23), 8721–8729 DOI: 10.1021/la300769d.
(110) Chu, H.; Johnson, N. R.; Mason, N. S.; Wang, Y. A [polycation:heparin] complex releases growth factors with enhanced bioactivity. *J. Controlled Release* **2011**, *150* (2), 157–163 DOI: 10.1016/j.jconrel.2010.11.025.
(111) Filatova, L. Y.; Donovan, D. M.; Becker, S. C.; Lebedev, D. N.; Priyma, A. D.; Koudriachova, H. V.; Kabanov, A. V.; Klyachko, N. L. Physicochemical characterization of the staphylolytic LysK enzyme in complexes with polycationic polymers as a potent antimicrobial. *Biochimie* **2013**, *95* (9), 1689–1696 DOI: 10.1016/j.biochi.2013.04.013.
(112) Insua, I.; Liamas, E.; Zhang, Z.; Peacock, A.; Krachler, A. M.; Fernandez-Trillo, F. Enzyme-responsive polyion complex (PIC) nanoparticles for the targeted delivery of antimicrobial polymers. *Polym. Chem.* **2016**, *7*, 2684–2690 DOI: 10.1039/C6PY00146G.
(113) Wang, B.; Jin, T.; Xu, Q.; Liu, H.; Ye, Z.; Chen, H. Direct loading and tunable release of antibiotics from polyelectrolyte multilayers to reduce bacterial adhesion and biofilm formation. *Bioconjugate Chem.* **2016**, *27* (5), 1305–1313 DOI: 10.1021/acs.bioconjchem.6b00118.
(114) Fan, Y.; Tang, S.; Thomas, E. L.; Olsen, B. D. Responsive block copolymer photonics triggered by protein–polyelectrolyte coacervation. *ACS Nano* **2014**, *8* (11), 11467–11473 DOI: 10.1021/nn504565r.
(115) Wang, J.; Velders, A. H.; Gianolio, E.; Aime, S.; Vergeldt, F. J.; Van As, H.; Yan, Y.; Drechsler, M.; de Keizer, A.; Cohen Stuart, M. A.; et al. Controlled mixing of lanthanide(iii) ions in coacervate core micelles. *Chem. Commun.* **2013**, *49* (36), 3736–3738 DOI: 10.1039/c3cc39148e.
(116) Miura, Y.; Tsuji, A. B.; Sugyo, A.; Sudo, H.; Aoki, I.; Inubushi, M.; Yashiro, M.; Hirakawa, K.; Cabral,

H.; Nishiyama, N.; et al. Polymeric micelle platform for multimodal tomographic imaging to detect scirrhous gastric cancer. *ACS Biomater. Sci. Eng.* **2015**, *1* (11), 1067–1076 DOI: 10.1021/acsbiomaterials.5b00142.

(117) Gao, G.; Yan, Y.; Pispas, S.; Yao, P. Sustained and extended release with structural and activity recovery of lysozyme from complexes with sodium (sulfamate carboxylate) isoprene/ethylene oxide block copolymer. *Macromol. Biosci.* **2010**, *10* (2), 139–146 DOI: 10.1002/mabi.200900186.

(118) Priftis, D.; Xia, X.; Margossian, K. O.; Perry, S. L.; Leon, L.; Qin, J.; de Pablo, J. J.; Tirrell, M. Ternary, tunable polyelectrolyte complex fluids driven by complex coacervation. *Macromolecules* **2014**, *47* (9), 3076–3085 DOI: 10.1021/ma500245j.

(119) Priftis, D.; Megley, K.; Laugel, N.; Tirrell, M. Complex coacervation of poly(ethylene-imine)/polypeptide aqueous solutions: thermodynamic and rheological characterization. *J. Colloid Interface Sci.* **2013**, *398* (C), 39–50 DOI: 10.1016/j.jcis.2013.01.055.

(120) Chollakup, R.; Smitthipong, W.; Eisenbach, C. D.; Tirrell, M. Phase behavior and coacervation of aqueous poly(acrylic acid)−poly(allylamine) solutions. *Macromolecules* **2010**, *43* (5), 2518–2528 DOI: 10.1021/ma902144k.

(121) Chollakup, R.; Beck, J. B.; Dirnberger, K.; Tirrell, M.; Eisenbach, C. D. Polyelectrolyte molecular weight and salt effects on the phase behavior and coacervation of aqueous solutions of poly(acrylic acid) sodium salt and poly(allylamine) hydrochloride. *Macromolecules* **2013**, *46* (6), 2376–2390 DOI: 10.1021/ma202172q.

(122) Priftis, D.; Tirrell, M. Phase behaviour and complex coacervation of aqueous polypeptide solutions. *Soft Matter* **2012**, *8* (36), 9396–9405 DOI: 10.1039/C2SM25604E.

(123) Priftis, D.; Laugel, N.; Tirrell, M. Thermodynamic characterization of polypeptide complex coacervation. *Langmuir* **2012**, *28* (45), 15947–15957 DOI: 10.1021/la302729r.

(124) Kayitmazer, A. B.; Koksal, A. F.; Iyilik, E. K. Complex coacervation of hyaluronic acid and chitosan: effects of pH, ionic strength, charge density, chain length and the charge ratio. *Soft Matter* **2015**, *11*, 8605–8612 DOI: 10.1039/C5SM01829C.

(125) Du, X.; Dubin, P. L.; Hoagland, D. A.; Sun, L. Protein-selective coacervation with hyaluronic acid. *Biomacromolecules* **2014**, *15* (3), 726–734 DOI: 10.1021/bm500041a.

(126) Sing, C. E. Development of the modern theory of polymeric complex coacervation. *Adv. Colloid Interface Sci.* **2016**, InPress DOI: 10.1016/j.cis.2016.04.004.

(127) Pak, C. W.; Kosno, M.; Holehouse, A. S.; Padrick, S. B.; Mittal, A.; Ali, R.; Yunus, A. A.; Liu, D. R.; Pappu, R. V.; Rosen, M. K. Sequence determinants of intracellular phase separation by complex coacervation of a disordered protein. *Mol. Cell* **2016**, *63* (1), 72–85 DOI: 10.1016/j.molcel.2016.05.042.

(128) Flanagan, S. E.; Malanowski, A. J.; Kizilay, E.; Seeman, D.; Dubin, P. L.; Donato-Capel, L.; Bovetto, L.; Schmitt, C. Complex equilibria, speciation, and heteroprotein coacervation of lactoferrin and β-lactoglobulin. *Langmuir* **2015**, *31* (5), 1776–1783 DOI: 10.1021/la504020e.

(129) van der Gucht, J.; Spruijt, E.; Lemmers, M.; Cohen Stuart, M. A. Polyelectrolyte complexes: bulk phases and colloidal systems. *J. Colloid Interface Sci.* **2011**, *361* (2), 407–422 DOI: 10.1016/j.jcis.2011.05.080.

(130) de Kruif, C. G.; Weinbreck, F.; de Vries, R. Complex coacervation of proteins and anionic polysaccharides. *Curr. Opin. Colloid Interface Sci.* **2004**, *9* (5), 340–349 DOI: 10.1016/j.cocis.2004.09.006.

(131) Kayitmazer, A. B.; Seeman, D.; Minsky, B. B.; Dubin, P. L.; Xu, Y. Protein–polyelectrolyte interactions. *Soft Matter* **2013**, *9* (9), 2553–2583 DOI: 10.1039/c2sm27002a.

(132) Harada, A.; Kataoka, K. Chain Length Recognition: Core-shell supramolecular assembly from oppositely charged block copolymers. *Science* **1999**, *283* (5398), 65–67 DOI: 10.1126/science.283.5398.65.

(133) Spruijt, E.; Westphal, A. H.; Borst, J. W.; Cohen Stuart, M. A.; van der Gucht, J. Binodal compositions of polyelectrolyte complexes. *Macromolecules* **2010**, *43* (15), 6476–6484 DOI: 10.1021/ma101031t.

(134) Spruijt, E.; Cohen Stuart, M. A.; van der Gucht, J. Linear viscoelasticity of polyelectrolyte complex coacervates. *Macromolecules* **2013**, *46* (4), 1633–1641 DOI: 10.1021/ma301730n.

(135) Spruijt, E.; Leermakers, F. A. M.; Fokkink, R.; Schweins, R.; van Well, A. A.; Cohen Stuart, M. A.; van der Gucht, J. Structure and dynamics of polyelectrolyte complex coacervates studied by scattering of neutrons, X-rays, and light. *Macromolecules* **2013**, *46* (11), 4596–4605 DOI: 10.1021/ma400132s.

(136) Anema, S. G.; de Kruif, C. G. K. Coacervates of lysozyme and β-casein. *J. Colloid Interface Sci.* **2013**, *398* (C), 255–261 DOI: 10.1016/j.jcis.2013.02.013.
(137) Anema, S. G.; Kees de Kruif, C. G. Co-acervates of lactoferrin and caseins. *Soft Matter* **2012**, *8* (16), 4471–4478 DOI: 10.1039/c2sm00015f.
(138) Anema, S. G.; de Kruif, C. G. K. Complex coacervates of lactotransferrin and β-lactoglobulin. *J. Colloid Interface Sci.* **2014**, *430* (C), 214–220 DOI: 10.1016/j.jcis.2014.05.036.
(139) de Kruif, C. G. K.; Pedersen, J.; Huppertz, T.; Anema, S. G. Coacervates of lactotransferrin and β- or κ-casein: structure determined using SAXS. *Langmuir* **2013**, *29* (33), 10483–10490 DOI: 10.1021/la402236f.
(140) Yan, Y.; Kizilay, E.; Seeman, D.; Flanagan, S.; Dubin, P. L.; Bovetto, L.; Donato, L.; Schmitt, C. Heteroprotein complex coacervation: bovine β-lactoglobulin and lactoferrin. *Langmuir* **2013**, *29* (50), 15614–15623 DOI: 10.1021/la4027464.
(141) Kayitmazer, A. B.; Strand, S. P.; Tribet, C.; Jaeger, W.; Dubin, P. L. Effect of polyelectrolyte structure on protein−polyelectrolyte coacervates: coacervates of bovine serum albumin with poly(diallyldimethylammonium chloride) versus chitosan. *Biomacromolecules* **2007**, *8* (11), 3568–3577 DOI: 10.1021/bm700645t.
(142) Xia, J.; Mattison, K.; Romano, V.; Dubin, P. L.; Muhoberac, B. B. Complexation of trypsin and alcohol dehydrogenase with poly(diallyldimethylammonium chloride). *Biopolymers* **1997**, *41* (4), 359–365 DOI: 10.1002/(SICI)1097-0282(19970405)41:4<359::AID-BIP1>3.0.CO;2-L.
(143) Cooper, C. L.; Goulding, A.; Kayitmazer, A. B.; Ulrich, S.; Stoll, S.; Turksen, S.; Yusa, S.-I.; Kumar, A.; Dubin, P. L. Effects of polyelectrolyte chain stiffness, charge mobility, and charge sequences on binding to proteins and micelles. *Biomacromolecules* **2006**, *7* (4), 1025–1035 DOI: 10.1021/bm050592j.
(144) Bohidar, H.; Dubin, P. L.; Majhi, P. R.; Tribet, C.; Jaeger, W. Effects of protein−polyelectrolyte affinity and polyelectrolyte molecular weight on dynamic properties of bovine serum albumin−poly(diallyldimethylammonium chloride) coacervates. *Biomacromolecules* **2005**, *6* (3), 1573–1585 DOI: 10.1021/bm049174p.
(145) Cooper, C. L.; Dubin, P. L.; Kayitmazer, A. B.; Turksen, S. Polyelectrolyte–protein complexes. *Curr. Opin. Colloid Interface Sci.* **2005**, *10* (1-2), 52–78 DOI: 10.1016/j.cocis.2005.05.007.
(146) Kizilay, E.; Seeman, D.; Yan, Y.; Du, X.; Dubin, P. L.; Donato-Capel, L.; Bovetto, L.; Schmitt, C. Structure of bovine β-lactoglobulin–lactoferrin coacervates. *Soft Matter* **2014**, *10*, 7262–7268 DOI: 10.1039/C4SM01333F.
(147) Lindhoud, S.; Voorhaar, L.; de Vries, R.; Schweins, R.; Cohen Stuart, M. A.; Norde, W. Salt-induced disintegration of lysozyme-containing polyelectrolyte complex micelles. *Langmuir* **2009**, *25* (19), 11425–11430 DOI: 10.1021/la901591p.
(148) Cohen Stuart, M. A.; Besseling, N. A. M.; Fokkink, R. G. Formation of micelles with complex coacervate cores. *Langmuir* **1998**, *14* (24), 6846–6849 DOI: 10.1021/la980778m.
(149) Tekaat, M.; tergerds, D. B. X.; nhoff, M. S. X.; Fery, A.; Cramer, C. Scaling properties of the shear modulus of polyelectrolyte complex coacervates: a time-pH superposition principle. *Phys. Chem. Chem. Phys.* **2015**, *17*, 22552–22556 DOI: 10.1039/C5CP02940F.
(150) Rawat, K.; Bohidar, H. B. Coacervation in biopolymers. *J. Phys. Chem. Biophys.* **2014**, *4* (165), 1000165 DOI: 10.4172/2161-0398.1000165.
(151) van der Kooij, H. M.; Spruijt, E.; Voets, I. K.; Fokkink, R.; Cohen Stuart, M. A.; van der Gucht, J. On the stability and morphology of complex coacervate core micelles: from spherical to wormlike micelles. *Langmuir* **2012**, *28* (40), 14180–14191 DOI: 10.1021/la303211b.
(152) Spruijt, E.; Sprakel, J.; Cohen Stuart, M. A.; van der Gucht, J. Interfacial tension between a complex coacervate phase and its coexisting aqueous phase. *Soft Matter* **2010**, *6* (1), 172–178 DOI: 10.1039/B911541B.
(153) Spruijt, E.; Sprakel, J.; Lemmers, M.; Cohen Stuart, M. A.; van der Gucht, J. Relaxation dynamics at different time scales in electrostatic complexes: time-salt superposition. *Phys. Rev. Lett.* **2010**, *105* (20), 208301–208304 DOI: 10.1103/PhysRevLett.105.208301.
(154) Dubin, P. L.; Gao, J.; Mattison, K. Protein purification by selective phase separation with polyelectrolytes. *Separation & Purification Reviews* **1994**, *23* (1), 1–16 DOI: 10.1080/03602549408001288.
(155) Xu, Y.; Mazzawi, M.; Chen, K.; Sun, L.; Dubin, P. L. Protein purification by polyelectrolyte coacervation: influence of protein charge anisotropy on selectivity. *Biomacromolecules* **2011**, *12* (5), 1512–1522 DOI: 10.1021/bm101465y.

(156) Kayitmazer, A. B.; Bohidar, H. B.; Mattison, K. W.; Bose, A.; Sarkar, J.; Hashidzume, A.; Russo, P. S.; Jaeger, W.; Dubin, P. L. Mesophase separation and probe dynamics in protein–polyelectrolyte coacervates. *Soft Matter* **2007**, *3* (8), 1064–1076 DOI: 10.1039/B701334E.
(157) Kayitmazer, A. B.; Quinn, B.; Kimura, K.; Ryan, G. L.; Tate, A. J.; Pink, D. A.; Dubin, P. L. Protein specificity of charged aequences in polyanions and heparins. *Biomacromolecules* **2010**, *11* (12), 3325–3331 DOI: 10.1021/bm1008074.
(158) Comert, F.; Malanowski, A. J.; Azarikia, F.; Dubin, P. L. Coacervation and precipitation in polysaccharide-protein systems. *Soft Matter* **2016**, *12*, 4154–4161 DOI: 10.1039/C6SM00044D.
(159) Antonov, M.; Mazzawi, M.; Dubin, P. L. Entering and exiting the protein−polyelectrolyte coacervate phase via nonmonotonic salt dependence of critical conditions. *Biomacromolecules* **2010**, *11* (1), 51–59 DOI: 10.1021/bm900886k.
(160) Hattori, T.; Kimura, K.; Seyrek, E.; Dubin, P. L. Binding of bovine serum albumin to heparin determined by turbidimetric titration and frontal analysis continuous capillary electrophoresis. *Anal. Biochem.* **2001**, *295* (2), 158–167 DOI: 10.1006/abio.2001.5129.
(161) Kaibara, K.; Okazaki, T.; Bohidar, H. B.; Dubin, P. L. pH-Induced coacervation in complexes of bovine serum albumin and cationic polyelectrolytes. *Biomacromolecules* **2000**, *1* (1), 100–107 DOI: 10.1021/bm990006k.
(162) Qin, J.; Priftis, D.; Farina, R.; Perry, S. L.; Leon, L.; Whitmer, J.; Hoffmann, K.; Tirrell, M.; de Pablo, J. J. Interfacial tension of polyelectrolyte complex coacervate phases. *ACS Macro Lett.* **2014**, *3* (6), 565–568 DOI: 10.1021/mz500190w.
(163) Fu, J.; Schlenoff, J. B. Driving forces for oppositely charged polyion association in aqueous solutions: Enthalpic, entropic, but not electrostatic. *JACS* **2016**, *138* (3), 980–990 DOI: 10.1021/jacs.5b11878.
(164) Lawrence, P. G.; Lapitsky, Y. Ionically cross-linked poly(allylamine) as a stimulus-responsive underwater adhesive: Ionic strength and pH effects. *Langmuir* **2015**, *31*, 1564–1574 DOI: 10.1021/la504611x.
(165) Laaser, J. E.; Jiang, Y.; Sprouse, D.; Reineke, T. M.; Lodge, T. P. pH- and ionic-strength-induced contraction of polybasic micelles in buffered aqueous solutions. *Macromolecules* **2015**, *48* (8), 2677–2685 DOI: 10.1021/acs.macromol.5b00360.
(166) Bae, Y.; Fukushima, S.; Harada, A.; Kataoka, K. Design of environment-sensitive supramolecular assemblies for intracellular drug delivery: polymeric micelles that are responsive to intracellular pH change. *Angew. Chem. Int. Ed.* **2003**, *42* (38), 4640–4643 DOI: 10.1002/anie.200250653.
(167) Nigen, M.; Croguennec, T.; Bouhallab, S. Formation and stability of α-lactalbumin–lysozyme spherical particles: Involvement of electrostatic forces. *Food Hydrocolloids* **2009**, *23* (2), 510–518 DOI: 10.1016/j.foodhyd.2008.02.005.
(168) Kunz, W.; Nostro, Lo, P.; Ninham, B. W. The present state of affairs with Hofmeister effects. *Curr. Opin. Colloid Interface Sci.* **2004**, *9* (1-2), 1–18 DOI: 10.1016/j.cocis.2004.05.004.
(169) Zhang, Y.; Cremer, P. S. Interactions between macromolecules and ions: the Hofmeister series. *Curr. Opin. Chem. Biol.* **2006**, *10* (6), 658–663 DOI: 10.1016/j.cbpa.2006.09.020.
(170) Pearson, R. G. Hard and soft acids and bases. *JACS* **1963**, *85* (22), 3533–3539 DOI: 10.1021/ja00905a001.
(171) Pearson, R. G. Hard and soft acids and bases, HSAB, part 1: fundamental principles. *J. Chem. Educ.* **1968**, *45* (9), 581–587 DOI: 10.1021/ed045p581.
(172) Collins, K. D. Ion hydration: implications for cellular function, polyelectrolytes, and protein crystallization. *Biophys. Chem.* **2006**, *119* (3), 271–281 DOI: 10.1016/j.bpc.2005.08.010.
(173) Collins, K. D. Charge density-dependent strength of hydration and biological structure. *Biophys. J.* **1997**, *72* (1), 65–76 DOI: 10.1016/S0006-3495(97)78647-8.
(174) Collins, K. D. Ions from the Hofmeister Series and Osmolytes: Effects on proteins in solution and in the crystallization process. *Methods* **2004**, *34* (3), 300–311 DOI: 10.1016/j.ymeth.2004.03.021.
(175) Rawat, K.; Aswal, V. K.; Bohidar, H. B. DNA–gelatin complex coacervation, UCST and first-order phase transition of coacervate to anisotropic ion gel in 1-methyl-3-octylimidazolium chloride ionic liquid solutions. *J. Phys. Chem. B* **2012**, *116* (51), 14805–14816 DOI: 10.1021/jp3102089.
(176) Biesheuvel, P. M.; Lindhoud, S.; de Vries, R.; Cohen Stuart, M. A. Phase behavior of mixtures of oppositely charged nanoparticles: heterogeneous Poisson−Boltzmann cell model applied to lysozyme and succinylated lysozyme. *Langmuir* **2006**, *22* (3), 1291–1300 DOI: 10.1021/la052334d.
(177) Koga, T.; Tanaka, F.; Motokawa, R.; Koizumi, S.; Winnik, F. M. Theoretical modeling of associated structures in aqueous solutions of hydrophobically modified telechelic PNIPAM nased on a neutron

scattering study. *Macromolecules* **2008**, *41* (23), 9413–9422 DOI: 10.1021/ma800957z.
(178) Liberatore, M. W.; Wyatt, N. B.; Henry, M.; Dubin, P. L.; Foun, E. Shear-induced phase separation in polyelectrolyte/mixed micelle coacervates. *Langmuir* **2009**, *25* (23), 13376–13383 DOI: 10.1021/la903260r.
(179) Perry, S. L.; Sing, C. E. PRISM-based theory of complex coacervation: excluded volume versus chain correlation. *Macromolecules* **2015**, *48* (14), 5040–5053 DOI: 10.1021/acs.macromol.5b01027.
(180) Turovsky, T.; Khalfin, R.; Kababya, S.; Schmidt, A.; Barenholz, Y.; Danino, D. Celecoxib encapsulation in β-casein micelles: Structure, interactions, and conformation. *Langmuir* **2015**, *31* (26), 7183–7192 DOI: 10.1021/acs.langmuir.5b01397.
(181) Rasente, R. Y.; Imperiale, J. C.; Lázaro-Martínez, J. M.; Gualco, L.; Oberkersch, R.; Sosnik, A.; Calabrese, G. C. Dermatan sulfate/chitosan polyelectrolyte complex with potential application in the treatment and diagnosis of vascular disease. *Carbohydr. Polym.* **2016**, *144*, 362–370 DOI: 10.1016/j.carbpol.2016.02.046.
(182) Wang, L.; Cao, Y.; Zhang, K.; Fang, Y.; Nishinari, K.; Phillips, G. O. Hydrogen bonding enhances the electrostatic complex coacervation between κ-carrageenan and gelatin. *Colloids Surf., A* **2015**, *482*, 604–610 DOI: 10.1016/j.colsurfa.2015.07.011.
(183) Chai, C.; Lee, J.; Huang, Q. The effect of ionic strength on the rheology of pH-induced bovine serum albumin κ-carrageenan coacervates. *LWT - Food Science and Technology* **2014**, *59* (1), 356–360 DOI: 10.1016/j.lwt.2014.05.024.
(184) Chremos, A.; Douglas, J. F. Counter-ion distribution around flexible polyelectrolytes having different molecular architecture. *Soft Matter* **2016**, *12*, 2932–2941 DOI: 10.1039/C5SM02873F.
(185) Laaser, J. E.; Jiang, Y.; Petersen, S. R.; Reineke, T. M.; Lodge, T. P. Interpolyelectrolyte complexes of polycationic micelles and linear polyanions: Structural stability and temporal evolution. *J. Phys. Chem. B* **2015**, *119* (52), 15919–15928 DOI: 10.1021/acs.jpcb.5b09010.
(186) Chuanoi, S.; Anraku, Y.; Hori, M.; Kishimura, A.; Kataoka, K. Fabrication of polyion complex vesicles with enhanced salt and temperature resistance and their potential applications as enzymatic nanoreactors. *Biomacromolecules* **2014**, *15* (7), 2389–2397 DOI: 10.1021/bm500127g.
(187) Lemmers, M.; Sprakel, J.; Voets, I. K.; van der Gucht, J.; Cohen Stuart, M. A. Multiresponsive reversible gels based on charge-driven assembly. *Angew. Chem.* **2009**, *122* (4), 720–723 DOI: 10.1002/ange.200905515.
(188) Krogstad, D. V. Investigating the structure-property relationships of aqueous self- assembled materials, 2012, pp 1–262.
(189) Anraku, Y.; Kishimura, A.; Yamasaki, Y.; Kataoka, K. Living unimodal growth of polyion complex vesicles via two-dimensional supramolecular polymerization. *JACS* **2013**, *135* (4), 1423–1429 DOI: 10.1021/ja3096587.
(190) Anraku, Y.; Kishimura, A.; Oba, M.; Yamasaki, Y.; Kataoka, K. Spontaneous formation of nanosized unilamellar polyion complex vesicles with tunable size and properties. *JACS* **2010**, *132* (5), 1631–1636 DOI: 10.1021/ja908350e.
(191) Mao, Z.; Cartier, R.; Hohl, A.; Farinacci, M.; Dorhoi, A.; Nguyen, T.-L.; Mulvaney, P.; Ralston, J.; Kaufmann, S. H. E.; Möhwald, H.; et al. Cells as factories for humanized encapsulation. *Nano Lett.* **2011**, *11* (5), 2152–2156 DOI: 10.1021/nl200801n.
(192) Bourouina, N.; Cohen Stuart, M. A.; Kleijn, J. M. Complex coacervate core micelles as diffusional nanoprobes. *Soft Matter* **2014**, *10* (2), 320–331 DOI: 10.1039/C3SM52245H.
(193) Bourouina, N.; de Kort, D. W.; Hoeben, F. J. M.; Janssen, H. M.; Van As, H.; Hohlbein, J.; van Duynhoven, J. P. M.; Kleijn, J. M. Complex coacervate core micelles with spectroscopic labels for diffusometric probing of biopolymer networks. *Langmuir* **2015**, *31* (46), 12635–12643 DOI: 10.1021/acs.langmuir.5b03496.
(194) Wu, B.-C.; Degner, B.; McClements, D. J. Soft matter strategies for controlling food texture: Formation of hydrogel particles by biopolymer complex coacervation. *J. Phys.: Condens. Matter* **2014**, *26* (46), 464104–464112 DOI: 10.1088/0953-8984/26/46/464104.
(195) Madene, A.; Jacquot, M.; Scher, J.; Desobry, S. Flavour encapsulation and controlled release - a review. *Int. J. Food Sci. Technol.* **2006**, *41* (1), 1–21 DOI: 10.1111/j.1365-2621.2005.00980.x.
(196) Augustin, M. A.; Hemar, Y. Nano- and micro-structured assemblies for encapsulation of food ingredients. *Chem. Soc. Rev.* **2009**, *38* (4), 902–912 DOI: 10.1039/B801739P.
(197) Johnson, N. R.; Wang, Y. Controlled delivery of heparin-binding EGF-like growth factor yields fast and comprehensive wound healing. *J. Controlled Release* **2013**, *166* (2), 124–129 DOI: 10.1016/j.jconrel.2012.11.004.

(198) McClements, D. J.; Decker, E. A.; Park, Y.; Weiss, J. Structural design principles for delivery of bioactive components in nutraceuticals and functional foods. *Crit. Rev. Food Sci. Nutr.* **2009**, *49* (6), 577–606 DOI: 10.1080/10408390902841529.
(199) McClements, D. J.; Li, Y. Structured emulsion-based delivery systems: controlling the digestion and release of lipophilic food components. *Adv. Colloid Interface Sci.* **2010**, *159* (2), 213–228 DOI: 10.1016/j.cis.2010.06.010.
(200) Truong-Le, V. L.; August, J. T.; Leong, K. W. Controlled gene delivery by DNA-gelatin nanospheres. *Hum. Gene. Ther.* **1998**, *9*, 1707–1717.
(201) Truong-Le, V. L.; Walsh, S. M.; Schweibert, E.; Mao, H.-Q.; Guggino, W. B.; August, J. T.; Leong, K. W. Gene transfer by DNA–gelatin nanospheres. *Arch. Biochem. Biophys.* **1999**, *361* (1), 47–56 DOI: 10.1006/abbi.1998.0975.
(202) Leong, K. W.; Mao, H. Q.; Truong-Le, V. L.; Roy, K.; Walsh, S. M.; August, J. T. DNA-polycation nanospheres as non-viral gene delivery vehicles. *J. Controlled Release* **1998**, *53* (1-3), 183–193 DOI: 10.1016/S0168-3659(97)00252-6.
(203) Ozbas-Turan, S.; Aral, C.; Kabasakal, L.; Keyer-Uysal, M.; Akbuga, J. Co-encapsulation of two plasmids in chitosan microspheres as a non-viral gene delivery vehicle. *J. Pharm. Pharm. Sci.* **2003**, *6* (1), 27–32.
(204) Thomasin, C.; Nam-Tran, H.; Merkle, H. P.; Gander, B. Drug microencapsulation by PLA/PLGA coacervation in the light of thermodynamics. 1. overview and theoretical considerations. *J. Pharm. Sci.* **1998**, *87* (3), 259–268 DOI: 10.1021/js970047r.
(205) Martin, N.; Li, M.; Mann, S. Selective uptake and refolding of globular proteins in coacervate microdroplets. *Langmuir* **2016**, *32* (23), 5881–5889 DOI: 10.1021/acs.langmuir.6b01271.
(206) Galan, A.; Ballester, P. Stabilization of reactive species by supramolecular encapsulation. *Chem. Soc. Rev.* **2016**, *45*, 1720–1737 DOI: 10.1039/C5CS00861A.
(207) Sedlák, E.; Fedunová, D.; Veselá, V.; Sedláková, D.; Antalík, M. Polyanion Hydrophobicity and protein basicity affect protein stability in protein−polyanion complexes. *Biomacromolecules* **2009**, *10* (9), 2533–2538 DOI: 10.1021/bm900480t.
(208) Khondee, S.; Olsen, C. M.; Zeng, Y.; Middaugh, C. R.; Berkland, C. Noncovalent PEGylation by polyanion complexation as a means to stabilize keratinocyte growth factor-2 (KGF-2). *Biomacromolecules* **2011**, *12* (11), 3880–3894 DOI: 10.1021/bm2007967.
(209) Tiwari, A.; Bindal, S.; Bohidar, H. B. Kinetics of protein−protein complex coacervation and biphasic release of salbutamol sulfate from coacervate matrix. *Biomacromolecules* **2009**, *10* (1), 184–189 DOI: 10.1021/bm801160s.
(210) Nishiyama, N.; Kataoka, K. Current state, achievements, and future prospects of polymeric micelles as nanocarriers for drug and gene delivery. *Pharmacol. Ther.* **2006**, *112* (3), 630–648 DOI: 10.1016/j.pharmthera.2006.05.006.
(211) Johnson, N. R.; Wang, Y. Coacervate delivery systems for proteins and small molecule drugs. *Expert Opin. Drug Delivery* **2014**, *11* (12), 1829–1832 DOI: 10.1517/17425247.2014.941355.
(212) Plummer, R.; Wilson, R. H.; Calvert, H.; Boddy, A. V.; Griffin, M.; Sludden, J.; Tilby, M. J.; Eatock, M.; Pearson, D. G.; Ottley, C. J.; et al. A phase I clinical study of cisplatin-incorporated polymeric micelles (NC-6004) in patients with solid tumours. *Br. J. Cancer* **2011**, *104* (4), 593–598 DOI: 10.1038/bjc.2011.6.
(213) Alsharabasy, A. M.; Moghannem, S. A.; El-Mazny, W. N. Physical preparation of alginate/chitosan polyelectrolyte complexes for biomedical applications. *J. Biomater. Appl.* **2016**, *30* (7), 1071–1079 DOI: 10.1177/0885328215613886.
(214) Li, H.; Johnson, N. R.; Usas, A.; Lu, A.; Poddar, M.; Wang, Y.; Huard, J. Sustained release of bone morphogenetic protein 2 via coacervate improves the osteogenic potential of muscle-derived stem cells. *Stem Cells Transl. Med.* **2013**, *2* (9), 667–677 DOI: 10.5966/sctm.2013-0027.
(215) Moore, K. W.; de Waal Malefyt, R.; Coffman, R. L.; OGarra, A. Interleukin-10 and the interleukin-10 receptor. *Annu. Rev. Immunol.* **2001**, *19* (1), 683–765 DOI: 10.1146/annurev.immunol.19.1.683.
(216) Ghobadi, A. F.; Letteri, R.; Parelkar, S. S.; Zhao, Y.; Chan-Seng, D.; Emrick, T.; Jayaraman, A. Dispersing zwitterions into comb polymers for nonviral transfection: Experiments and molecular simulation. *Biomacromolecules* **2016**, *17* (2), 546–557 DOI: 10.1021/acs.biomac.5b01462.
(217) Li, S.; Huang, L. Nonviral gene therapy: promises and challenges. *Gene Ther.* **2000**, *7* (1), 31–34 DOI: 10.1038/sj.gt.3301110.
(218) Chesnoy, S.; Huang, L. Structure and function of lipid-DNA complexes for gene delivery. *Annu. Rev. Biophys. Biomol. Struct.* **2000**, *29*, 27–47.

(219) Martin, B.; Sainlos, M.; Aissaoui, A.; Oudrhiri, N.; Hauchecorne, M.; Vigneron, J.; Lehn, J.; Lehn, P. The design of cationic lipids for gene delivery. *Curr. Pharm. Des.* **2005**, *11* (3), 375–394 DOI: 10.2174/1381612053382133.

(220) Katayose, S.; Kataoka, K. Remarkable increase in nuclease resistance of plasmid DNA through supramolecular assembly with poly(ethylene glycol). *J. Pharm. Sci.* **1998**, *87*, 160–163 DOI: 10.1021/js970304s.

(221) Katayose, S.; Kataoka, K. Water-soluble polyion complex associates of DNA and aoly(ethylene glycol)−aoly(L-lysine) Block copolymer. *Bioconjugate Chem.* **1997**, *8* (5), 702–707 DOI: 10.1021/bc9701306.

(222) Ainalem, M.-L.; Nylander, T. DNA condensation using cationic dendrimers—morphology and supramolecular structure of formed aggregates. *Soft Matter* **2011**, *7* (10), 4577–18 DOI: 10.1039/c0sm01171a.

(223) Cai, J.; Yue, Y.; Rui, D.; Zhang, Y.; Liu, S.; Wu, C. Effect of chain length on cytotoxicity and endocytosis of cationic polymers. *Macromolecules* **2011**, *44* (7), 2050–2057 DOI: 10.1021/ma102498g.

(224) Peng, H. T.; Shek, P. N. Novel wound sealants: biomaterials and applications. *Expert Rev. Med. Devices* **2014**, *7* (5), 639–659 DOI: 10.1586/erd.10.40.

(225) Wolfert, M. A.; Schacht, E. H.; Toncheva, V.; Ulbrich, K.; Nazarova, O.; Seymour, L. W. Characterization of vectors for gene therapy formed by self-assembly of DNA with synthetic block co-polymers. *Hum. Gene. Ther.* **1996**, *7* (17), 2123–2133 DOI: 10.1089/hum.1996.7.17-2123.

(226) Tangsangasaksri, M.; Takemoto, H.; Naito, M.; Maeda, Y.; Sueyoshi, D.; Kim, H. J.; Miura, Y.; Ahn, J.; Azuma, R.; Nishiyama, N.; et al. siRNA-loaded polyion complex micelle decorated with charge-conversional polymer tuned to undergo stepwise response to intra-tumoral and intra-rndosomal pHs for exerting enhanced RNAi efficacy. *Biomacromolecules* **2016**, *17* (1), 246–255 DOI: 10.1021/acs.biomac.5b01334.

(227) Stewart, R. J. Protein-based underwater adhesives and the prospects for their biotechnological production. *Appl. Microbiol. Biotechnol.* **2010**, *89* (1), 27–33 DOI: 10.1007/s00253-010-2913-8.

(228) Shao, H.; Stewart, R. J. Biomimetic underwater adhesives with environmentally triggered setting mechanisms. *Adv. Mater.* **2010**, *22* (6), 729–733 DOI: 10.1002/adma.200902380.

(229) Wei, W.; Tan, Y.; Rodriguez, N. R. M.; Yu, J.; Israelachvili, J. N.; Waite, J. H. A mussel-derived one component adhesive coacervate. *Acta Biomater.* **2014**, *10* (4), 1663–1670 DOI: 10.1016/j.actbio.2013.09.007.

(230) Zhang, L.; Lipik, V.; Miserez, A. Complex coacervates of oppositely charged co-polypeptides inspired by the sandcastle worm glue. *J. Mater. Chem. B* **2016**, *4*, 1544–1556 DOI: 10.1039/C5TB02298C.

(231) Maier, G. P.; Rapp, M. V.; Waite, J. H.; Israelachvili, J. N.; Butler, A. Adaptive synergy between catechol and lysine promotes wet adhesion by surface salt displacement. *Chem. Eng. News* **2015**, *349* (6248), 628–632 DOI: 10.1126/science.aab0556.

(232) Lam, J.; Clark, E. C.; Fong, E. L. S.; Lee, E. J.; Lu, S.; Tabata, Y.; Mikos, A. G. Evaluation of cell-laden polyelectrolyte hydrogels incorporating poly(l-Lysine) for applications in cartilage tissue engineering. *Biomaterials* **2016**, *83* (c), 332–346 DOI: 10.1016/j.biomaterials.2016.01.020.

(233) Wang, D.-A.; Varghese, S.; Sharma, B.; Strehin, I.; Fermanian, S.; Gorham, J.; Fairbrother, D. H.; Cascio, B.; Elisseeff, J. H. Multifunctional chondroitin sulphate for cartilage tissue–biomaterial integration. *Nat. Mater.* **2007**, *6* (5), 385–392 DOI: 10.1038/nmat1890.

(234) Jones, J. P.; Sima, M.; O'Hara, R. G.; Stewart, R. J. Water-borne endovascular embolics inspired by the undersea adhesive of marine sandcastle worms. *Adv. Healthcare Mater.* **2016**, *5* (7), 795–801 DOI: 10.1002/adhm.201500825.

(235) Kim, H. J.; Hwang, B. H.; Lim, S.; Choi, B.-H.; Kang, S. H.; Cha, H. J. Mussel adhesion-employed water-immiscible fluid bioadhesive for urinary fistula sealing. *Biomaterials* **2015**, *72*, 104–111 DOI: 10.1016/j.biomaterials.2015.08.055.

(236) Papanna, R.; Mann, L. K.; Tseng, S. C. G.; Stewart, R. J.; Kaur, S. S.; Swindle, M. M.; Kyriakides, T. R.; Tatevian, N.; Moise, K. J., Jr. Cryopreserved human amniotic membrane and a bioinspired underwater adhesive to seal and promote healing of iatrogenic fetal membrane defect sites. *Placenta* **2015**, *36* (8), 888–894 DOI: 10.1016/j.placenta.2015.05.015.

(237) Papanna, R.; Moise, K. J., Jr; Mann, L. K.; Fletcher, S.; Schniederjan, R.; Bhattacharjee, M. B.; Stewart, R. J.; Kaur, S.; Prabhu, S. P.; Tseng, S. C. G. Cryopreserved human umbilical cord patch for in-uterospina bifida repair. *Ultrasound Obstet Gynecol* **2016**, *47* (2), 168–176 DOI:

10.1002/uog.15790.
(238) Williams, D. S.; Patil, A. J.; Mann, S. Spontaneous structuration in coacervate-based protocells by polyoxometalate-mediated membrane assembly. *Small* **2014**, *10* (9), 1830–1840 DOI: 10.1002/smll.201303654.
(239) Yin, Y.; Niu, L.; Zhu, X.; Zhao, M.; Zhang, Z.; Mann, S.; Liang, D. Non-equilibrium behaviour in coacervate-based protocells under electric-field-induced excitation. *Nat. Commun.* **2016**, *7*, 10658 DOI: 10.1038/ncomms10658.
(240) Monnard, P.-A.; Walde, P. Current ideas about prebiological compartmentalization. *Life* **2015**, *5* (2), 1239–1263 DOI: 10.3390/life5021239.
(241) Mann, S. The origins of life: old problems, new chemistries. *Angew. Chem. Int. Ed.* **2012**, *52* (1), 155–162 DOI: 10.1002/anie.201204968.
(242) Keating, C. D. Aqueous phase separation as a possible route to compartmentalization of biological molecules. *Acc. Chem. Res.* **2012**, *45* (12), 2114–2124 DOI: 10.1021/ar200294y.
(243) Dominak, L. M.; Gundermann, E. L.; Keating, C. D. Microcompartmentation in artificial cells: pH-induced conformational changes alter protein localization. *Langmuir* **2010**, *26* (8), 5697–5705 DOI: 10.1021/la903800e.
(244) Long, M. S.; Jones, C. D.; Helfrich, M. R.; Mangeney-Slavin, L. K.; Keating, C. D. Dynamic microcompartmentation in synthetic cells. *PNAS* **2005**, *102* (17), 5920–5925 DOI: 10.1073/pnas.0409333102.
(245) Kolb, V. M.; Swanson, M.; Menger, F. M. Coacervates as prebiotic chemical reactors; Hoover, R. B., Levin, G. V., Rozanov, A. Y., Eds.; SPIE, 2012; Vol. 8521, p 85210E.
(246) Oparin, A. I. The origin of primary colloidal systems. In *The Origin of Life*; 1953; pp 137–162.
(247) Menger, F. M.; Sykes, B. M. Anatomy of a Coacervate. *Langmuir* **1998**, *14* (15), 4131–4137 DOI: 10.1021/la980208m.
(248) Devi, N.; Sarmah, M.; Khatun, B.; Maji, T. K. Encapsulation of active ingredients in polysaccharide-protein complex coacervates. *Adv. Colloid Interface Sci.* **2016**, InPress DOI: 10.1016/j.cis.2016.05.009.
(249) Szostak, J. W.; Bartel, D. P.; Luisi, P. L. Synthesizing life. *Nature* **2001**, *409*, 387–390 DOI: 10.1038/35053176.
(250) Aumiller, W. M., Jr; Keating, C. D. Experimental models for dynamic compartmentalization of biomolecules in liquid organelles: Reversible formation and partitioning in aqueous biphasic systems. *Adv. Colloid Interface Sci.* **2016**, InPress DOI: 10.1016/j.cis.2016.06.011.
(251) Narayanaswamy, R.; Levy, M.; Tsechansky, M.; Stovall, G. M.; O'Connell, J. D.; Mirrielees, J.; Ellington, A. D.; Marcotte, E. M. Widespread reorganization of metabolic enzymes into reversible assemblies upon nutrient starvation. *PNAS* **2009**, *106* (25), 10147–10152 DOI: 10.1073/pnas.0812771106.
(252) Feric, M.; Vaidya, N.; Harmon, T. S.; Mitrea, D. M.; Zhu, L.; Richardson, T. M.; Kriwacki, R. W.; Pappu, R. V.; Brangwynne, C. P. Coexisting liquid phases underlie nucleolar subcompartments. *Cell* **2016**, *165* (7), 1686–1697 DOI: 10.1016/j.cell.2016.04.047.
(253) Nott, T. J.; Petsalaki, E.; Farber, P.; Jervis, D.; Fussner, E.; Plochowietz, A.; Craggs, T. D.; Bazett-Jones, D. P.; Pawson, T.; Forman-Kay, J. D.; et al. Phase transition of a disordered nuage protein generates environmentally responsive membraneless organelles. *Mol. Cell* **2015**, *57* (5), 936–947 DOI: 10.1016/j.molcel.2015.01.013.
(254) Stoeger, T.; Battich, N.; Pelkmans, L. Passive noise filtering by cellular compartmentalization. *Cell* **2016**, *164* (6), 1151–1161 DOI: 10.1016/j.cell.2016.02.005.
(255) Decher, G. Fuzzy Nanoassemblies: toward layered polymeric multicomposites. *Science* **1997**, *277* (5330), 1232–1237 DOI: 10.1126/science.277.5330.1232.
(256) JEWELL, C.; LYNN, D. Surface-mediated delivery of DNA: Cationic polymers take charge. *Curr. Opin. Colloid Interface Sci.* **2008**, *13* (6), 395–402 DOI: 10.1016/j.cocis.2008.03.005.
(257) Jewell, C. M.; Lynn, D. M. Multilayered polyelectrolyte assemblies as platforms for the delivery of DNA and other nucleic acid-based therapeutics. *Adv. Drug Delivery Rev.* **2008**, *60*, 979–999 DOI: 10.1016/j.addr.2008.02.010.
(258) Jewell, C. M.; Zhang, J.; Fredin, N. J.; Wolff, M. R.; Hacker, T. A.; Lynn, D. M. Release of plasmid DNA from intravascular stents coated with ultrathin multilayered polyelectrolyte films. *Biomacromolecules* **2006**, *7*, 2483–2491 DOI: 10.1021/bm0604808.
(259) Jewell, C. M.; Zhang, J.; Fredin, N. J.; Lynn, D. M. Multilayered polyelectrolyte films promote the direct and localized delivery of DNA to cells. *J. Controlled Release* **2005**, *106* (1-2), 214–223 DOI:

10.1016/j.jconrel.2005.04.014.
(260) Schaaf, P.; Schlenoff, J. B. Saloplastics: Processing compact polyelectrolyte complexes. *Adv. Mater.* **2015**, *27* (15), 2420–2432 DOI: 10.1002/adma.201500176.
(261) Hariri, H. H.; Schlenoff, J. B. Saloplastic macroporous polyelectrolyte complexes: cartilage mimics. *Macromolecules* **2010**, *43* (20), 8656–8663 DOI: 10.1021/ma1012978.
(262) Porcel, C. H.; Schlenoff, J. B. Compact polyelectrolyte complexes: “saloplastic” candidates for biomaterials. *Biomacromolecules* **2009**, *10* (11), 2968–2975 DOI: 10.1021/bm900373c.